Phase transitions and ferroelectricity in Mn hybrid: $MnCl_4(C_6H_5CH_2CH_2NH_3)_2$

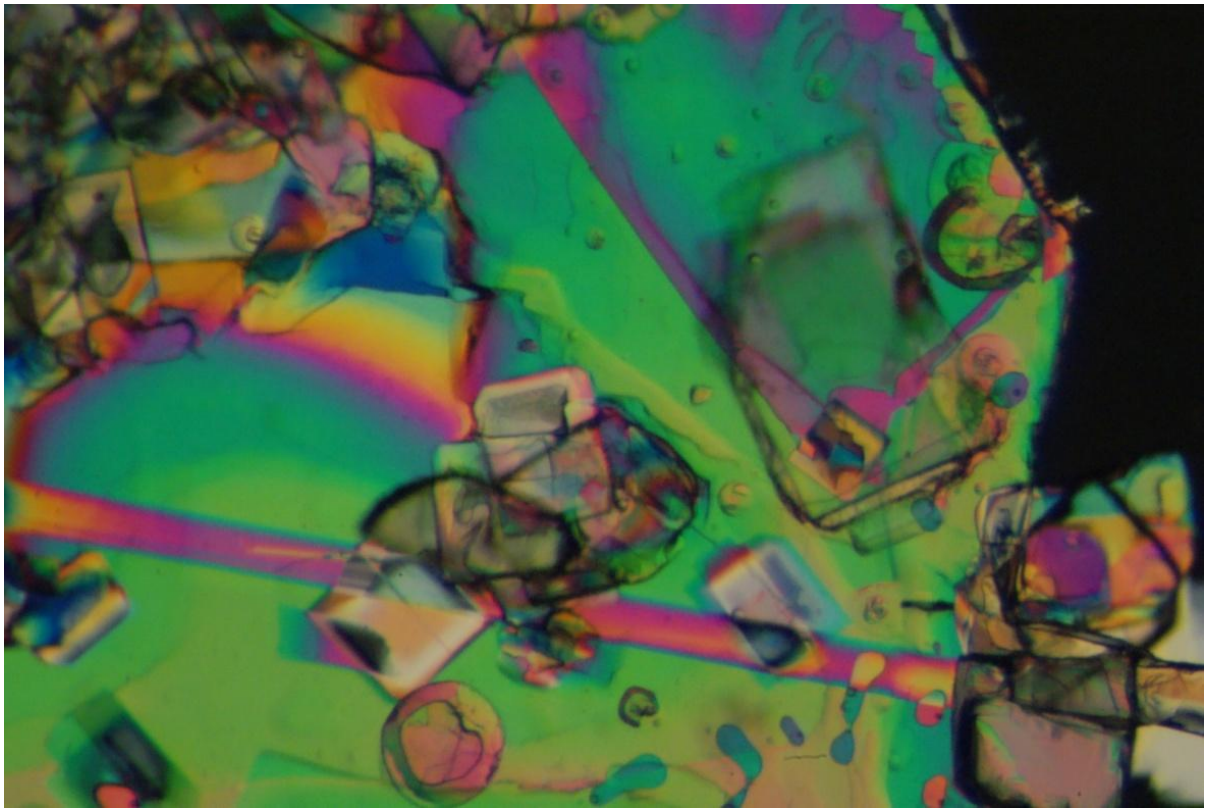

By Arnoud Everhardt
At Solid State Materials for Electronics group
Zernike Institute for Advanced Materials
Rijksuniversiteit Groningen

Bachelor project
Supervised by Anne Arkenbout and Thomas Palstra

July 28th, 2010

Contents

1. Introduction 2
2. Synthesis 7
3. Structure 9
4. Phase transitions..... 14
5. Birefringence..... 16
6. Temperature dependent X-ray..... 22
7. Capacitance 24
8. Pyroelectric 28
9. Conclusions..... 32
10. Literature..... 34

1. Introduction

Hybrids

Generally, a hybrid is a combination of two different components in the same system. Here, the term “hybrid” is used for inorganic-organic hybrid, which combines inorganic and organic components in one material. [1]

All elements are ordered in the periodic table, shown in **fig 1.1**. The organic elements are the elements in the red, with column 9 displaying the halogens which are also often used in organic materials. The inorganics are all the other elements (excluding hydrogen). The black circle gives the inorganics that are most widely used in hybrids because of their good magnetic and electric properties.

The macroscopic effects of inorganic materials are typically characterized by covalent and ionic interactions and they offer the potential for high carrier density and mobility, a wide range of band gaps, magnetic interactions, ferroelectric transitions and thermal stability. Organic materials typically have their macroscopic effects dominated by weaker interactions like hydrogen bonds and vanderwaals interactions. They provide nearly unlimited flexibility of structural diversity, good polarizability and they can also be made conductive. The aim of hybrid materials is to combine several of those properties from both the inorganics and the organics in one material, to produce useful combinations of those properties or even completely new phenomena. [2,3]

Hybrids can have several properties and applications. Useful properties can be molecular homogeneity, transparency, flexibility, durability [4], multiferroicity [6] and even new electronic and optical properties which do not belong to the organic and inorganic building blocks [5]. Several applications have already been found, including bonding of hydrogen [7], contact lenses, coatings [6], energy-storage applications, photovoltaics and sensors [8].

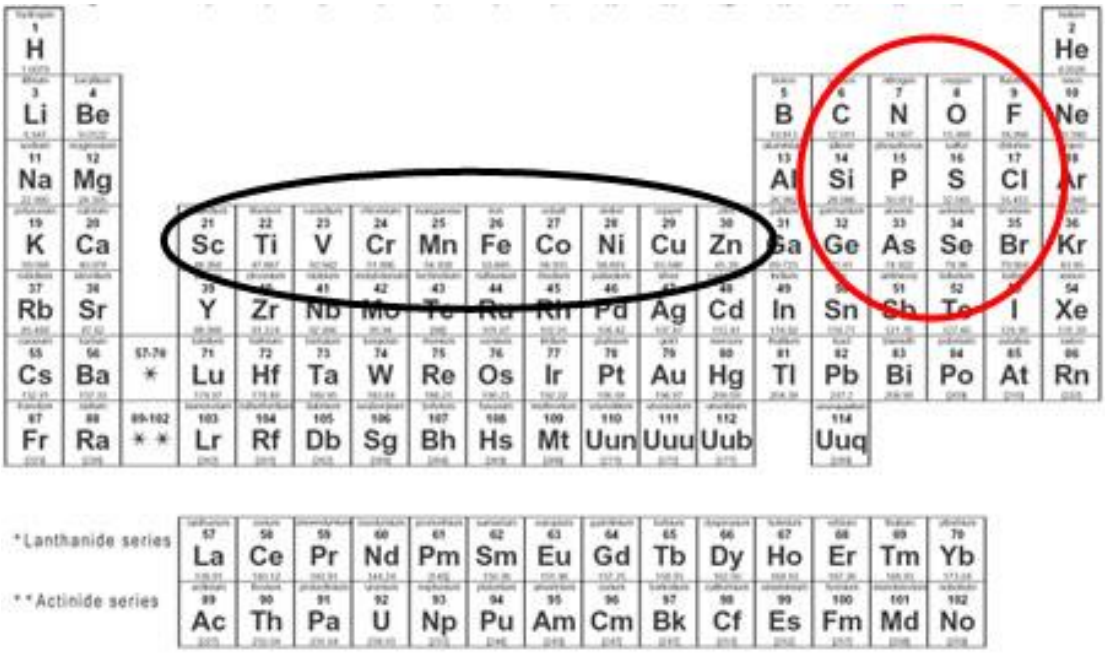

Fig 1.1 *Periodic table. The organics and halogens are given by the red circle; the inorganics are all the other elements. The black circle gives the inorganics commonly used in these hybrids.*

The hybrid investigated here is $MnCl_4(C_6H_5CH_2CH_2NH_3)_2$, bis(phenyl ethyl ammonium) tetrachloromanganate(II). There are several materials reported in literature which are similar to this material. The most interesting material is $CuCl_4(C_6H_5CH_2CH_2NH_3)_2$ [1], which has the same organic molecule and only differs in the metal. The research was inspired by this material and the aim of the research was to find out if some properties are similar.
More hybrids were found in literature, for example $[NH_3\text{-}(CH_2)_n\text{-}NH_3]MnCl_4$ and $[C_nH_{2n+1}NH_3]_2MCl_4$ (M is a metal) reported by Arend [9,10], which show several metals and different organic groups; $(C_4H_9NH_3)_2MI_4$, with iodide as the halogen and a different metal [3] and $(CH_3NH_3)HgCl_3$ [11]. Some of these hybrids will be compared to the hybrid of the research to find out similarities.

The general structure [3, 6, 10, 22] of most of these hybrids is very similar. The basic structure, as shown in **fig 1.2**, is composed of an inorganic layer of polyhedra with the organic molecules stacked in between. The polyhedron is an octahedron in nearly all cases. The polyhedron is composed of a metal in the middle with halogens ordered around the metal. The organic molecules have an ammonium group which interacts with the inorganic layer.
Even though the general structure of hybrids is usually very similar, with inorganic polyhedrons and organic molecules stacked in between, the organic layer can shown large structural diversity. Structures as shown in **fig 1.3** are also possible structures for hybrids.

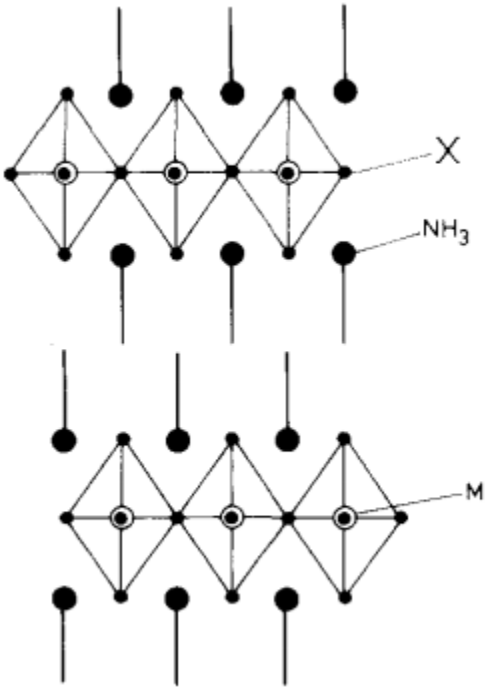

Fig 1.2 *[10] General structure of hybrids. Polyhedron around the metal M with halogens X, with organic layers in between NH_3-group at the end.*

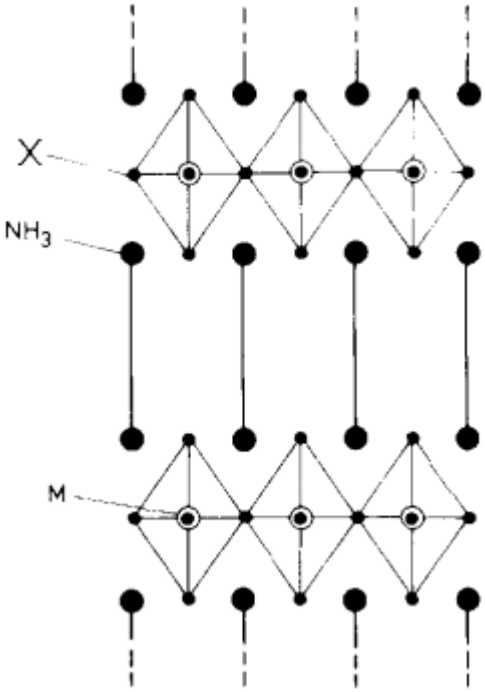

Fig 1.3 *[10] Another general structure hybrids can show.*

The first report that could be found on these kind of hybrids is from 1968 [12], and in the 1970's there were several reports on the synthesis and properties of these hybrids [9, 10, 13]. The structures were not yet called hybrids in those articles. Hybrids are currently a hot topic in research, as applications have been found and they have a potential to be a

new route to devices. The main current interest is the fact that hybrids can be multiferroic. [14]
Multiferroicity is the property that is investigated for the hybrid in this report, as there are clues this hybrid possesses this property.

Multiferroicity

Multiferroicity is the combination of two or more ferroic properties, like (anti)ferromagnetism, (anti)ferroelectricity and ferroelasticity. Here only (anti)ferromagnetism and (anti)ferroelectricity will be covered. [15] However, this combination is rarely seen in materials [14].
A material can be magnetically polarizable, electically polarizable, ferromagnetic, ferroelectric or any combination of those properties (**fig 1.4**) [16]. There is only little overlap in these properties.

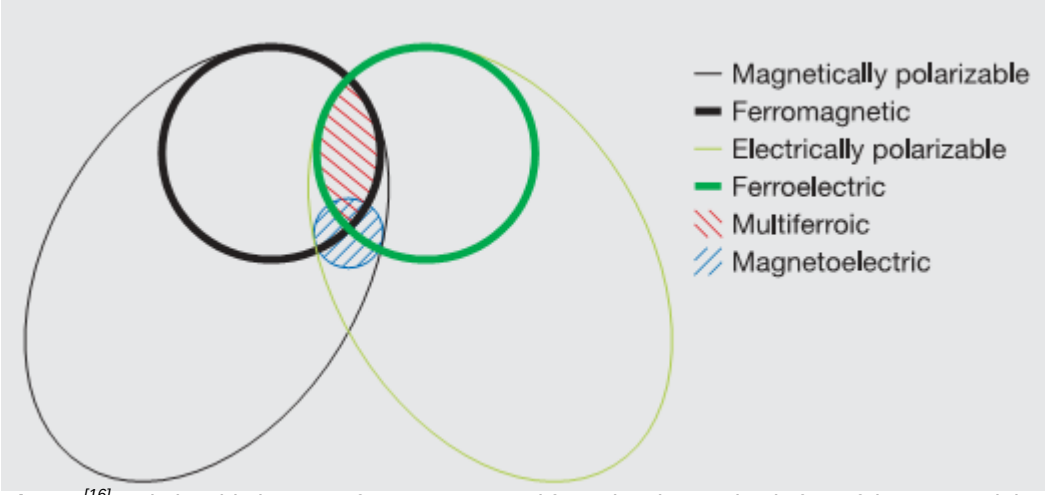

Fig 1.4 *[16] Relationship between ferromagnets and ferroelectrics, and only few of those materials are multiferroic.*

The properties (anti-)ferromagnetism and (anti-)ferroelectricity have a long-range ordening in the material and most of them show hysteresis: the response of the material depends on its history. [15]

Magnetism is commonly created by unpaired electrons. Electrons have a spin and the spin creates a magnetic dipole moment. In a ferromagnet, the spins of the electrons are aligned in the same direction (**fig 1.5**), causing a macroscopic magnetic moment to be observed. The orientation of those spins can be influenced by an external magnetic field (**fig 1.7**). Because of the ordening of the spins, even at no external field, there is still a magnetic moment. A large external field must be applied to change the complete magnetic moment of the material. In an antiferromagnet, the spins are anti-parallel aligned (**fig 1.6**). Even though there is no macroscopic magnetic moment to be observed, this property does show a long range order in the material so it is considered a ferroic property. [15]

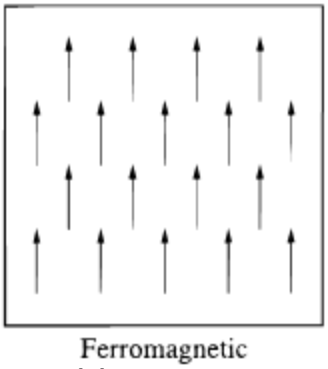

Fig 1.5 *[15] Spins in a ferromagnet are parallel aligned.*

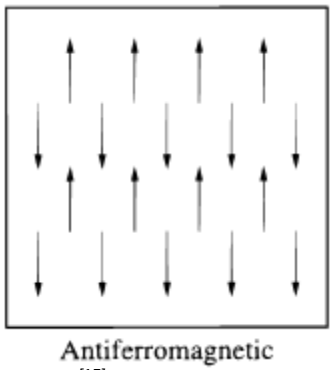

Fig 1.6 *[15] Spins in an antiferromagnet are anti-parallel aligned.*

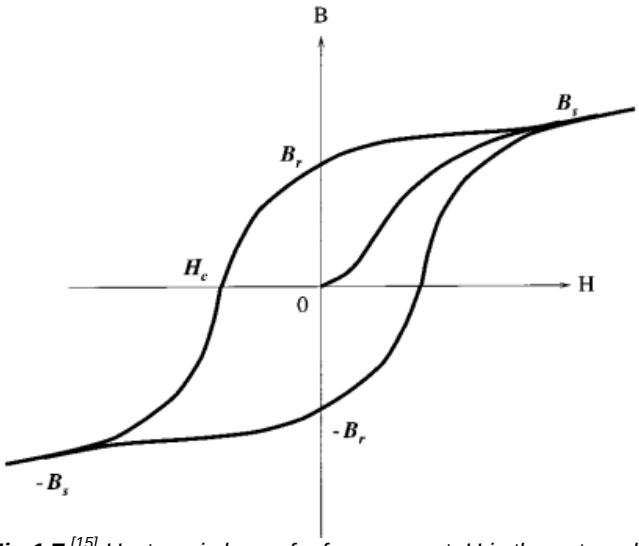

Fig 1.7 *[15] Hysteresis loop of a ferromagnet. H is the external magnetic field and B is the magnetization of the material.*

Ferroelectricity shows similar properties as a ferromagnet, with electricity instead of magnetism. The dipoles in a ferroelectric are parallel ordered in the material (**fig 1.8**), and the direction of the ordening can be influenced by an external electric field. At zero electric field, there is still a macroscopic polarisation in the material. It also shows hysteresis, shown in **fig 1.9**. [15]

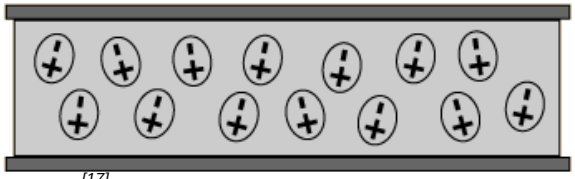

Fig 1.8 *[17] Ordering of the dipoles in a ferroelectric.*

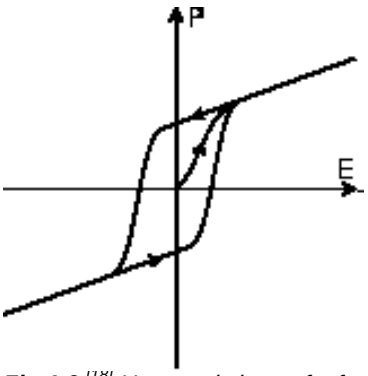

Fig 1.9 *[18] Hysteresis loop of a ferroelectric. E is the electric field, P the polarisation.*

In solid state, the usual cause of (anti-)ferroelectricity is a double potential well for an ion, as can be seen in **fig 1.10**. This double potential well requires a (charged) ion to be in one of the two wells, causing a charge buildup because of an off-centre displacement of an ion. In a ferromagnet the offset of the ions are parallel aligned and in an antiferromagnet they are anti-parallel aligned. [15]

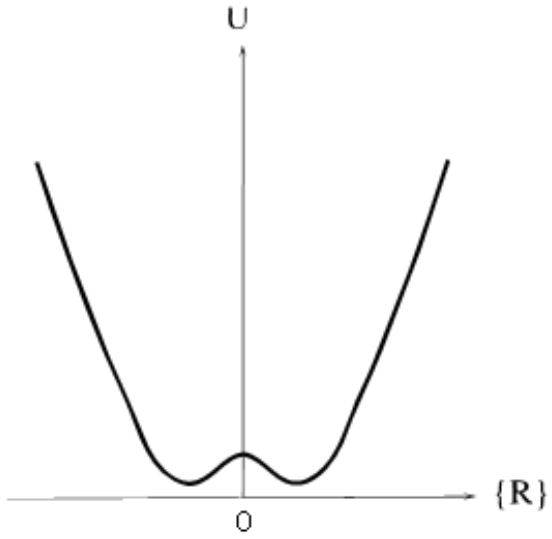

Fig 1.10 *[15] Double potential well for an (charged) ion. U is the potential energy and R is the distance from the centre.*

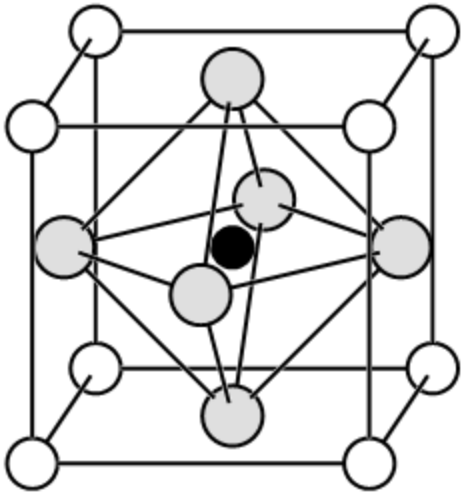

Fig 1.11 *[19] Structure of a conventional perovskite like $BaTiO_3$.*

In conventional perovskite materials, like $BaTiO_3$ (**fig 1.11**), the double potential well for ferroelectricity is caused by donation of 2p oxygen orbitals to the formally empty d-orbitals of the transition metal cation. This causes an offset of that cation. This gives the requirement that the transition metal cation must have empty d-orbitals. However, to have any magnetism in the material, the d-orbitals must be partially filled to have unpaired electrons. So in these conventional systems, the combination of ferromagnetism and ferroelectricity is forbidden. [15]

However, there are ways to circumvent this problem. Some ways to achieve that are to induce ferroelectricity in another way, like Coulomb-interaction or hydrogen bonds [5], or to use magnetic spirals [20].

Multiferroics are a hot topic in research as they have a potential to make data storage much faster and more efficient, by reading magnetically stored data electrically [21].

The Cu hybrid shows polarisation by hydrogen bonds and ferromagnetism by unpaired electrons in the transition metal. The polarisation could be a source of ferroelectricity (as it is one of the ways to get ferroelectricity in multiferroics), but it has not yet been proven for the Cu hybrid [1].

The Mn hybrid has been proven to be antiferromagnetic [1], and the aim of this research is to find out if the Mn hybrid is ferromagnetic, and thus proving it to be multiferroic. The way to do it is to take a look at the phase transitions and to investigate if they show polarisation. This polarisation could be a source of ferromagnetism.

2. Synthesis

The synthesis of $MnCl_4(C_6H_5CH_2CH_2NH_3)_2$ is a self assembly of manganese chloride ($MnCl_2$) and 2-phenylethylammoniumchloride ($C_6H_5CH_2CH_2NH_3Cl$). These two components are solved equimolarly in ethanol and they crystallize in the desired crystal structure.

First, the 2-phenylethylammoniumchloride salt has to be prepared (**fig 2.1**). 2-phenylethylamine was put into an erlenmeyer and concentrated hydrochloric acid was added by a pipette. This was added slowly because the reaction is exothermic. This mixture was stirred and cooled in a room temperature water bath. Yellow polycrystalline solid was formed. The reaction was finished when no more steam came from the reaction mixture on adding hydrochloric acid. The resulting solid was filtered, rinsed with small amounts of hydrochloric acid and washed with small amounts of ice-cooled water. The precipitate was dried overnight. The product was characterized by powder X-ray diffraction (chapter 3).

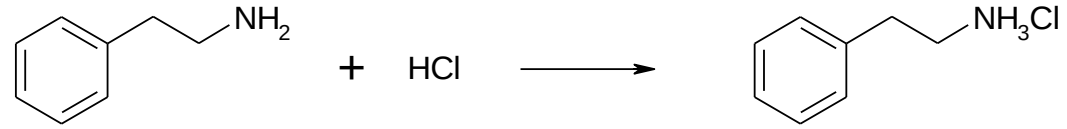

Fig 2.1 *Preparation of 2-phenylethylammonium chloride. 2-phenylethylammonia reacts with hydrochloric acid to form the product.*

The second step of the reaction, shown in **fig 2.2**, is the self assembly of the organic 2-phenylethylammonium chloride with the inorganic manganese(II)chloride. The dried yellow product was mixed with pink manganese(II)chloride powder and this mixture was solved in a solvent. This mixture was put in an erlenmeyer with aluminium foil on top with just two small holes in it (**fig 2.3**). This was put into the oven at 50-60 °C until all solvent was evaporated.
When pure ethanol was used as a solvent, the reactants did not dissolve completely and produced a suspension. On the top of the suspension, small colourless crystals (**fig 2.4**) were formed. When 80% ethanol and 20% water was used as a solvent, the reactants dissolved completely and much larger crystals (up to 1cm, shown in **fig 2.5**) were obtained. In pure water, the reactants did not form a product. The reaction works best with ethanol, but some water is required for complete solvation.
The product was characterised by X-ray diffraction (chapter 3) and confirmed the formation of the Mn hybrid.
The evaporation rate is very important in this process, because when the solution was allowed to evaporate faster (in a beaker glass), powder Mn hybrid was formed. The evaporation rate has to be very small.

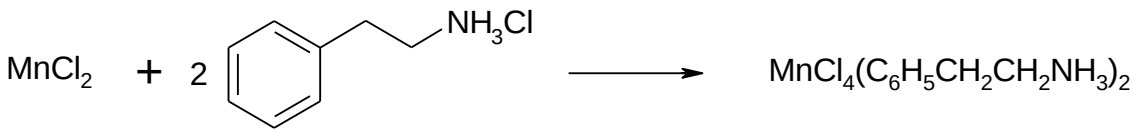

Fig 2.2 *Reaction of 2-phenylethylammonium chloride with manganese(II)chloride is a self assembly of the two components.*

Fig 2.3 *Setup of the evaporation of the solvent: an erlenmeyer with aluminium foil and two small holes (shown by the arrows) in the aluminium.*

Fig 2.4 *Crystal of the Mn hybrid on mm paper.*

Fig 2.5 *Crystals of the Mn hybrid prepared from 20% water and 80% ethanol.*

3. Structure

Phenylethylammonium chloride

The organic molecule (phenylethylammonium chloride) in the hybrid is a solid and its crystal structure has been resolved by single-crystal X-ray diffraction (see **fig 3.1**) [22]. It was characterized by powder X-ray diffraction and that spectrum is compared to the calculated spectrum from the known structure. In **fig 3.2**, the comparison is given. The red spectrum is the calculated one and the black spectrum is the measured one. It can be seen that all observable reflections are shown in both spectra, with the intensities also nearly equal. Only at 5 º and 33 º, the intensity of the observed spectrum is much higher. These peaks correspond to {00x} planes, so they are planes that are perpendicular to the c-axis. The fact that these peaks have higher intensity, comes from preferred orientation [23]: the bonds in the c-direction are weaker, so in a powder spectrum, these planes are more often cleaved than other planes. That results in a higher intensity for those planes. So it can be concluded that phenylethylammonium chloride was formed with purity up to the detection limit of X-ray in the first step of the synthesis.

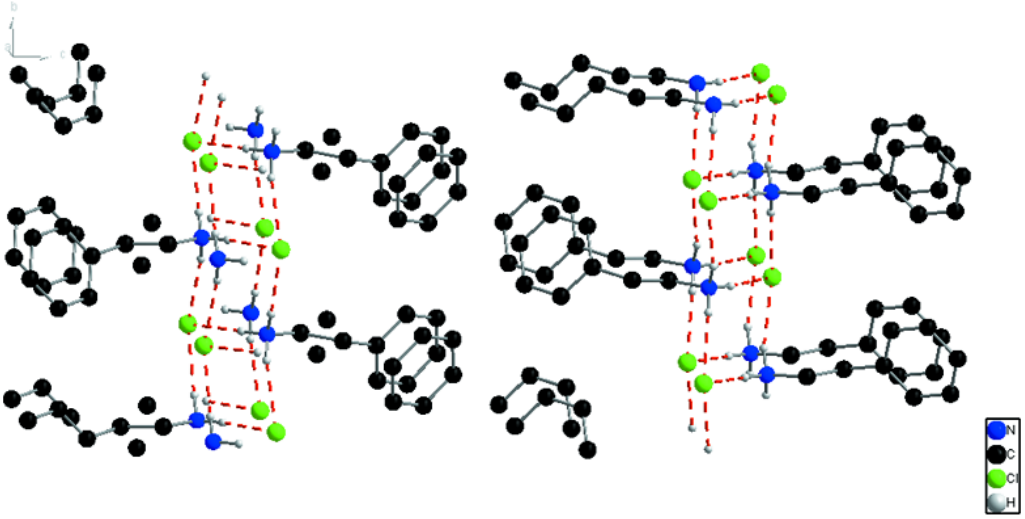

Fig 3.1 *[22] Crystal structure of phenylethylammonium chloride.*

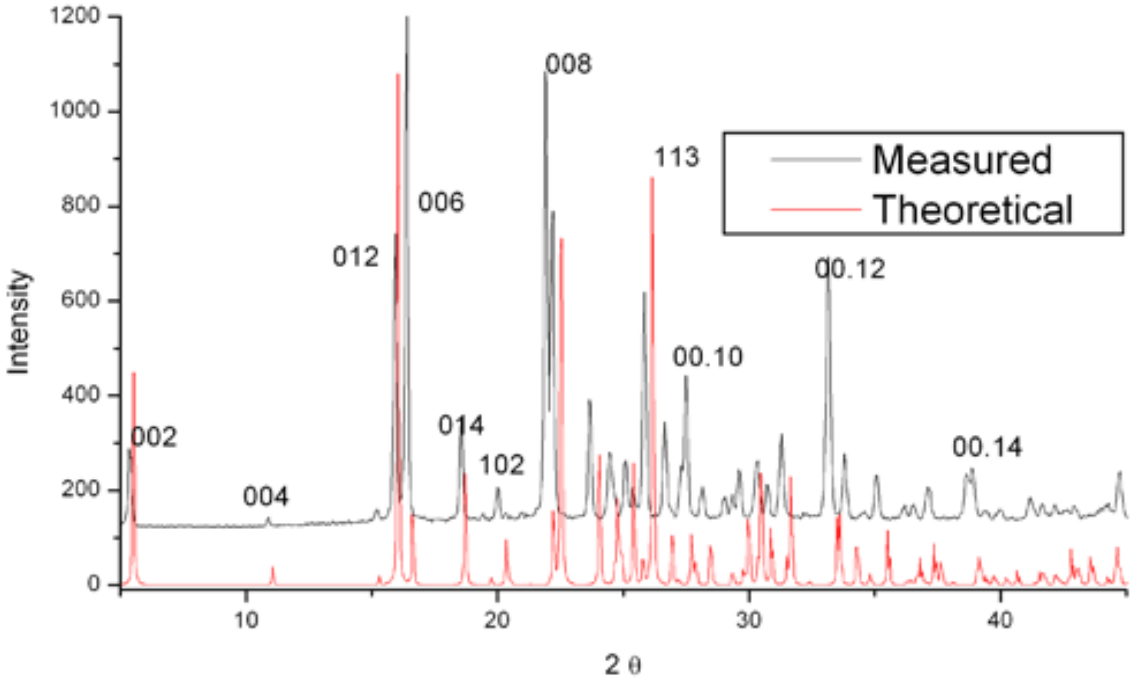

Fig 3.2 *Powder X-ray spectra of phenylethylammonium chloride, black is measured and red is calculated.*

Mn hybrid

The crystal structure of the hybrid is resolved by single-crystal X-ray diffraction and the structure is shown in **fig 3.3**. The structure is an inorganic layer of octahedra with the organic molecules packed in between. The ammonium-groups ($R\text{-}NH_3$) are pointing towards the inorganic layers, and the hydrogens of those ammonium-groups give hydrogen bonding with the inorganic layer (as can be seen at fig **3.3b**). This structure is the same as the schematically drawn general hybrid from **fig 1.2**.
An interesting fact that can be seen in this structure, is that the inorganic polyhedra are buckled in the a-axis. This buckling could be a source for a double potential well (**fig 1.10**) for polarisation like in the Cu hybrid [1]. The double potential well is created because the buckling destroys the symmetry in the environment for the nitrogens, so its hydrogens have to form a hydrogen bond into one direction or into the other. So this material has a potential to be polar.

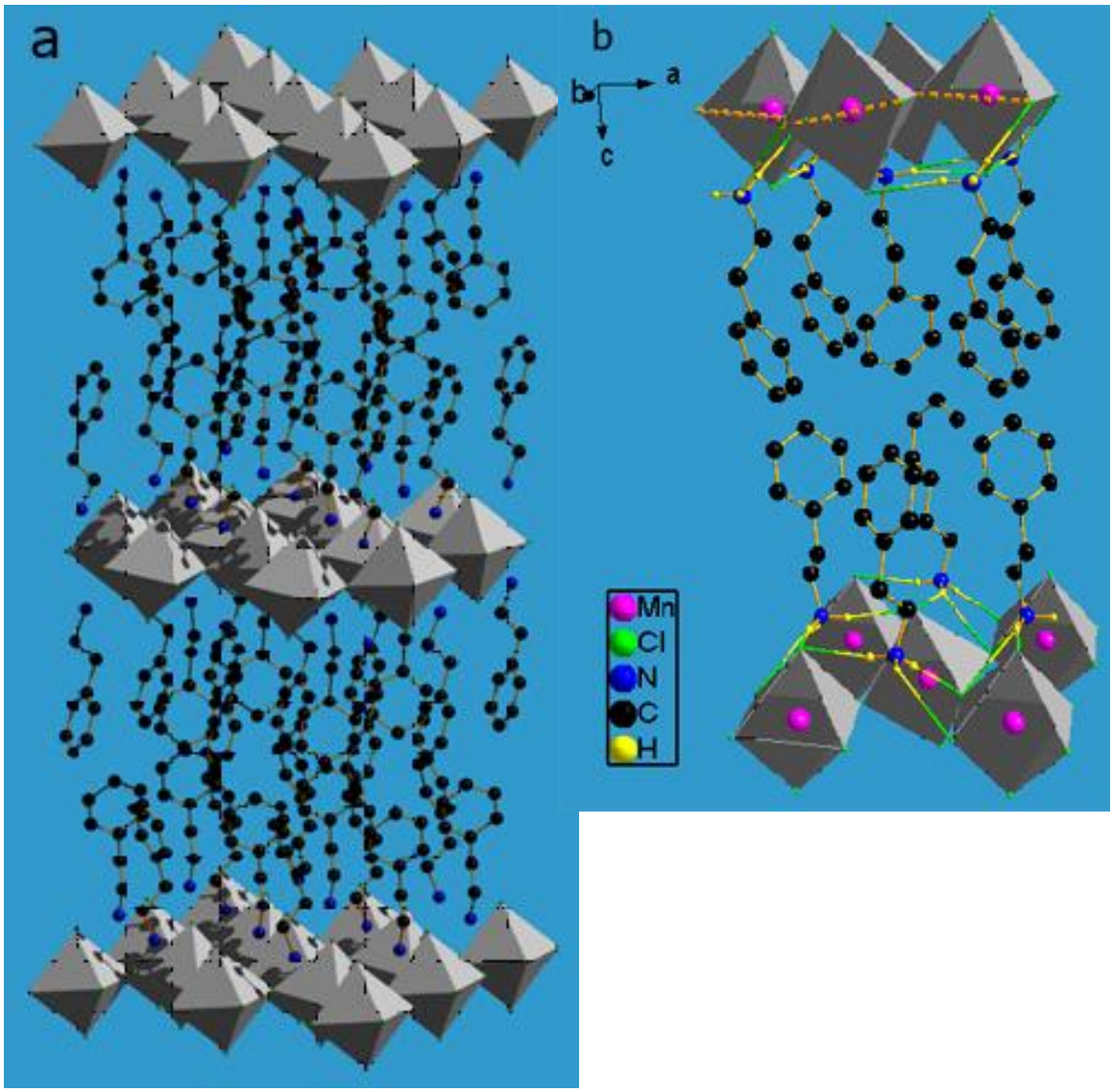

Fig 3.3 *Crystal structure of the Mn hybrid. a gives an overview of the crystal, b gives a close up including the hydrogen bonds. In b, the buckling in the a-axis is showed by the dashed orange bonds, which make angles with each other. This buckling is not seen in the b-axis.*

The product formed after the synthesis was characterized by powder X-ray diffraction and that spectrum was compared to the calculated spectrum from this structure in **fig 3.4**. All reflections observed in these spectra correspond to each other, where the reflections at 13 º, 23 º, 27 º, 37 º, 41 º and 44 º (all on 2θ) have an higher intensity in the measured spectrum due to preferred orientation of the {00x} planes [24]. The intensities do not correspond very well, but that is not a major problem since there is so much preferred orientation. The reflective positions correspond, so the conclusion can be drawn that the Mn hybrid is formed, with any possible impurities below the detection limit of the X-ray.

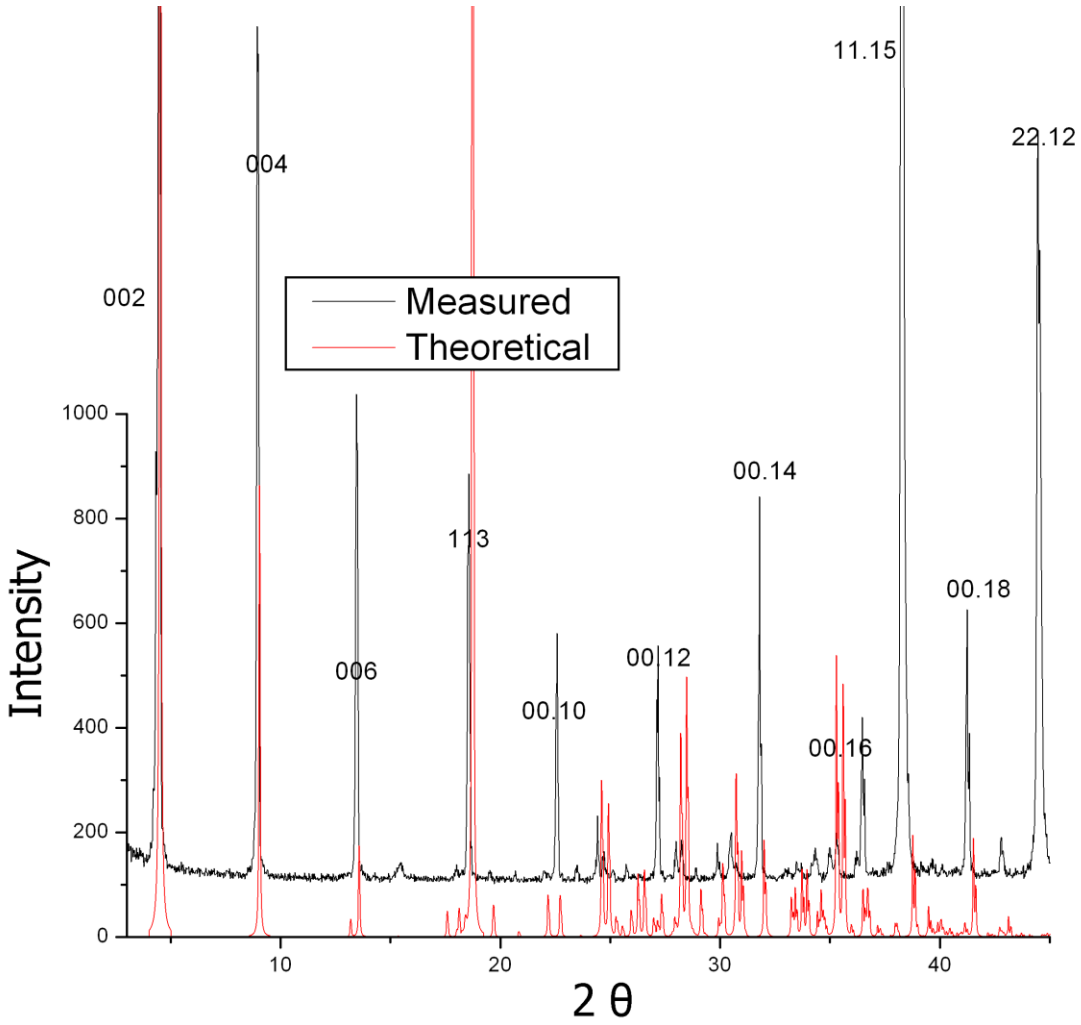

Fig 3.4 *Powder X-ray spectra of Mn hybrid, black is measured and red is calculated. The number at the reflections are the reflection planes.*

Other hybrids

The structure of the Mn hybrid is very similar to the Cu hybrid (**fig 3.5**) with the same organic molecules. This material also has a buckling and it is polar due to this buckling, so the Mn hybrid has a good chance to be polar as well. [1]

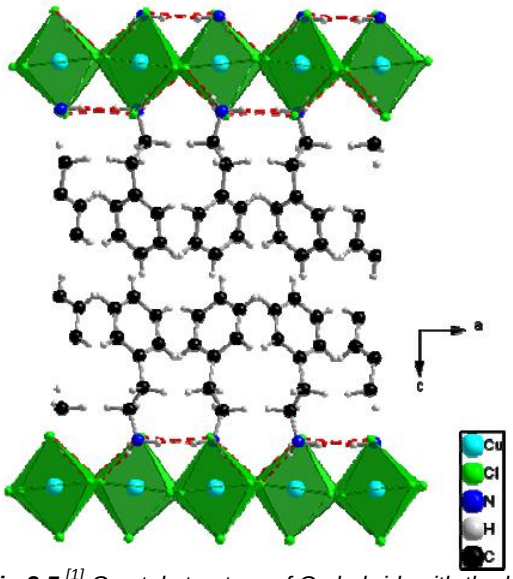

Fig 3.5 *[1] Crystal structure of Cu hybrid, with the buckling of the octahedra.*

4. Phase transitions

Phase transition can be first order or second order. This classification is based on the derivative of the chemical potential. If the first derivative of a thermodynamic variable is discontinuous, the phase transition is first order. If the second derivative is discontinous, the phase transition is second order (see **fig 4.1**). [25]

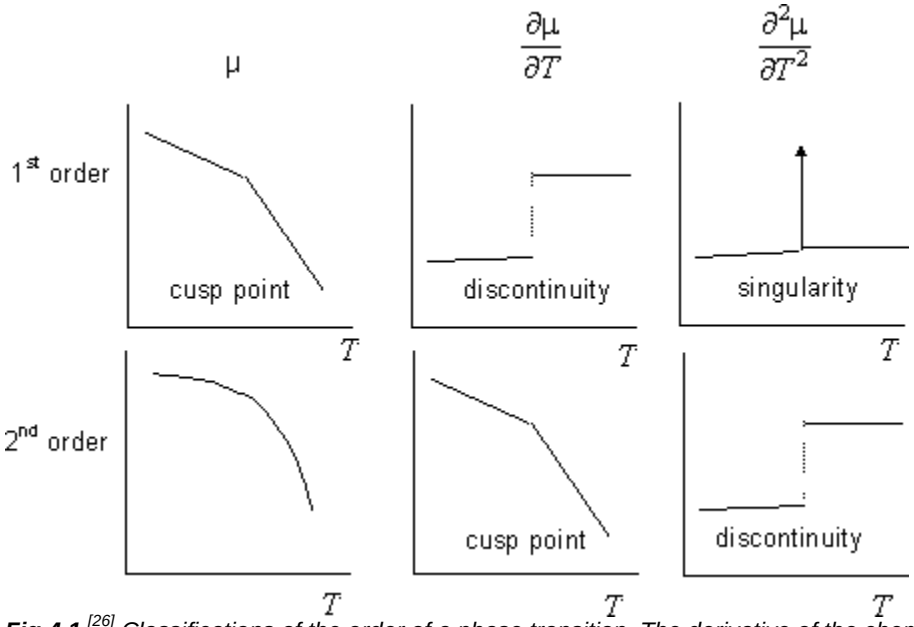

Fig 4.1 *[26] Classifications of the order of a phase transition. The derivative of the chemical potential is taken and if the first derivative is discontinous, it is a first order transition; if the second derivative is discontinuous, it is a second order transition.*

The phase transitions for a material can be found using Differential Scanning Calorimetry (DSC). This is a technique that registers the amount of heat required to heat the sample 1 degree Celcius. This heat flow is the heat capacity of the sample, which is the second derivative of the chemical potential (**fig 4.1**). At a phase transition, the amount of heat required will be higher or lower than the original value because a transition must be made (incorporating a change in the enthalpy, ΔH). So a peak is observed at a phase transition. [27]

The DSC measurement for the Mn hybrid is shown in **fig 4.2**. Two phase transitions can be seen, at 94-95 ºC and at 143-144 ºC. At higher temperatures (from 180 ºC) the material degraded as the mass went down, and at lower temperatures (down to -50 ºC) no phase transitions could be observed.
The phase transition at 144 ºC is a first order phase transition. The heat capacity shows a singularity just as in **fig 4.1**. The area under the peak is the the heat required for the phase transition, the latent heat. The latent heat for this phase transition is 0.054 W/G.[27]
The phase transition at 95 ºC is a second order phase transition, because it shows a discontinuity at the phase transition just as in **fig 4.1**. At lower temperatures than the transition, relaxation occurs so the parameter continuously changes to some value. This phase transition has no latent heat, so the area under the curve does not mean anything. There seems to be a hysteresis effect in the DSC measurement as the transition occurs one degree lower when cooling than when heating. This small hysteresis is probably due to external effects, such as a delay effect in the measurement of the temperature.

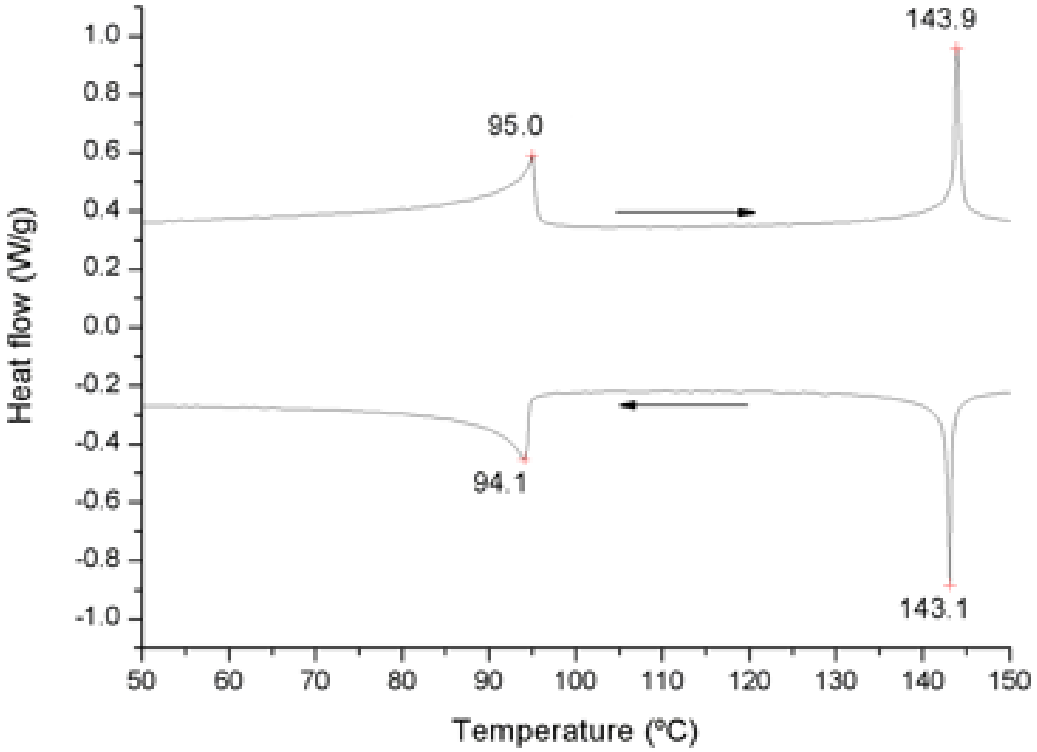

Fig 4.2 *DSC measurement of the Mn hybrid, upper curve is on heating, lower curve is on cooling. Two phase transitions can be seen, at 94-95 ºC and at 143-144 ºC. The measurement is done at a Universal V2.5H TA Instruments and performed by Gert Alberda van Ekenstein. The mass didn't change significantly during the experiment.*

The Cu-hybrid has three phase transitions, two that are first order and one that is second order. The polar phase transition is at 70 ºC and is first-order. [1] The hybrid $(C_2H_5NH_3)_2ZnBr_4$ has a first-order transition and $(C_4H_9NH_3)_2ZnBr_4$ has a second-order transition, so the order of the transition can be changed by something as small as a longer alkyl-chain [28]. In hybrids of the kind $(C_nH_{2n+1}NH_3)_2MCl_4$ with M = Mn and Cu, only second-order transitions were observed, where chain melting was the cause of the transitions [29].

For a ferroelectric phase transition, both first-order [30] as second-order [31] transitions have been reported. So both phase transitions can potentially be a ferroelectric transition.

5. Birefringence

The Mn hybrid is crystalline, with three crystal axes in the material as shown in **fig 5.1**. The crystal grows in three dimensions, but the interactions in the c-direction are much weaker than in the a- and b-directions, so the macroscopic crystal is much longer in the a- and b-directions than in the c-direction, giving flat rectangulae as macroscopic crystals.

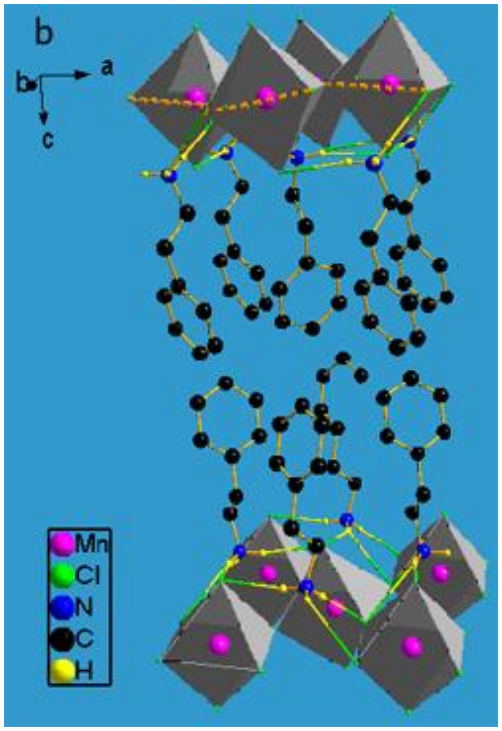

Fig 5.1 *Crystal structure of Mn hybrid.*

Birefringence is the decomposition of light into two different rays when it passes through anisotropic materials. Light is a transverse wave (**fig 5.2**) with the electric field oscilating perpendicular to the direction of motion. When the direction of motion is parallel to one axis of the crystal (in the Mn hybrid: the c-axis), the electric field interacts with the other two axes (in the Mn hybrid: a- and b-axes). If a material is anisotropic, the axes are different, so the interaction of the electric field with the axes is also different. The light interacts with matter through the fractive index (n), so if that parameter is different for the material in the axes, it can show birefringence. The refractive index determines the retardation of the light through the material, so in one of the axes the light is retarded more than in the other axis, which produces two different rays.

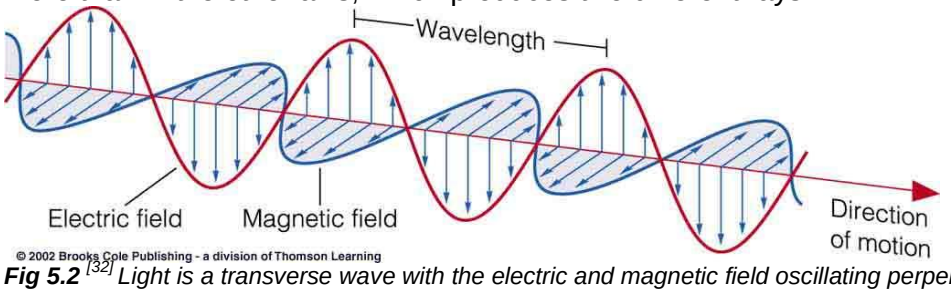

Fig 5.2 [32] *Light is a transverse wave with the electric and magnetic field oscillating perpendicular to the direction of motion. The magnetic field is neglected as its effects are much smaller than the electric field.*

Birefringence is used as an analytical method to obtain structural data from the crystal. The setup used in given in **fig 5.3**. Linearly polarized light is coming into the crystal, parallel to the c-axis. This light is decomposed in two different rays and this light is taken through a polarizer to again produce linearly polarized light. The linearly polarized light can interact differently with the a- than with the b-axis, while the interaction with the c-axis is the same

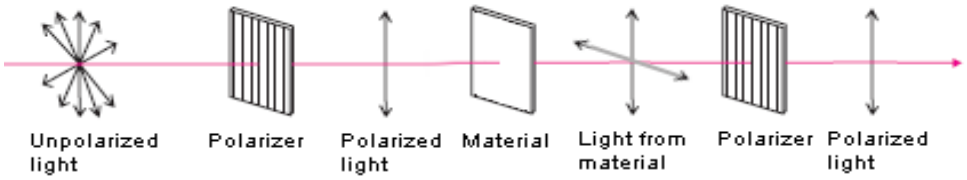

Fig 5.3 *Setup used in the analytical birefringence. Unpolarized light goes through a polarizer to produce linearly polarized light, the material decomposes the light into two beams and this is taken through a polarizer to produce linearly polarized light again.*

The Mn hybrid is anisotropic as all three axes are different from each other, so it can show birefringence. The light is coming parallel to the c-axis, so the a- and b-axes are observed in this method.

The mechanism of birefringence is displayed in **fig 5.4**, with the results displayed in **fig 5.5**. In **fig 5.4a** the incoming electric field is oriented parallel to the a-axis, so there is no interaction at all the the b-axis. One ray is going out that didn't have any changes, so it is white (**fig 5.5a**). In **fig 5.4b**, the crystal is rotated 90 º, so there is interaction with the b-axis, but no interaction with the a-axis and that produces the same result as given in fig **5.5a**.
Another way to orient the crystal and the polarisation is by letting the linearly polarized light have an angle of 90 º with the polarizer, giving cross-polarisation. The background will appear black, as no light can pass it. When one of the crystal axes is parallel to the electric field, the crystal will also appear black, as if nothing is changed in the crystal. This is shown in **fig 5.4c** and **fig 5.5b**.
The most interesting cases are given by **fig 5.4d** and **fig 5.4e**. The polarisation makes an angle with the crystal axes, so the electric field interacts with both axes. The incoming light is projected on the a- and the b-axes, producing two different rays. Those rays are shown in **fig 5.6a**, with the red and blue rays (which for simplicity is assumed to be the a- and b-axis rays, but it could also be the other way around). While the light goes through the air, the rays are kept together. But once they enter the crystal (the grey area), the blue ray is retarded more than the red ray. When the light goes out of the crystal, one of the rays has a certain retardation with respect to the other. When they hit the polarizer, the component of the ray parallel to the polarizer is taken and they give interference. Because some information is lost on the polarizer (only the parallel parts of the rays are taken), white light will not return, but colours are shown.
The projection on the polarizer of the projection of the light on the a- and b-axis determines the birefringence. In **fig 5.4d** and **fig 5.6a** this is different from **fig 5.4e** and **fig 5.6b**. The projection of the a-axis on the polarizer has the same direction in both cases. But the projection of the b-axis on the polarizer is different, as the direction of the projection on the polarizer is different in those cases. In **fig 5.4d** and **fig 5.6a**, the light that will be projected on the polarizer has the same phase when entering the crystal. In **fig 5.4e** and **fig 5.6b**, that light is exactly out of phase. So at the interference, those two cases produce exactly opposite interference, thus leading to complementary colours.

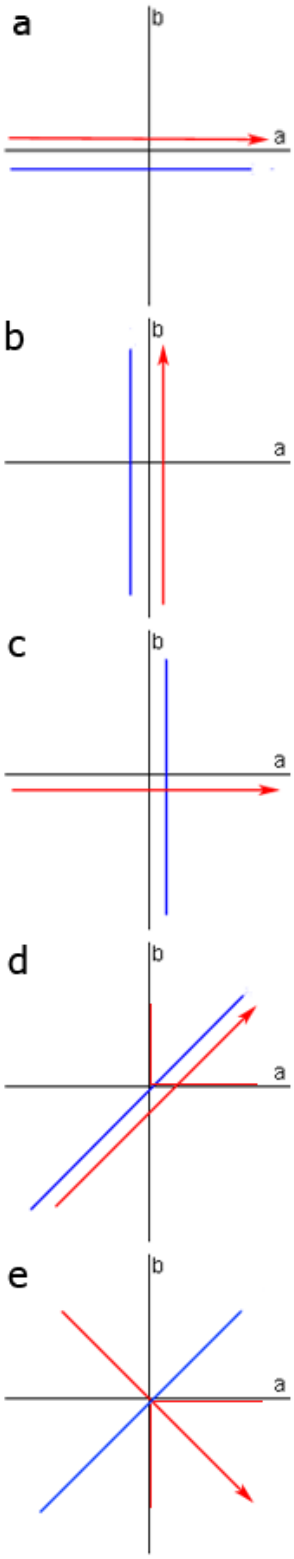

Fig 5.4 *The axes a and b are the crystal axes, the red arrow is the polarisation of the incoming light and the blue line is the polarisation of the polarizer after the material. In d and e, the projection of the light on the a- and b-axes are shown.*

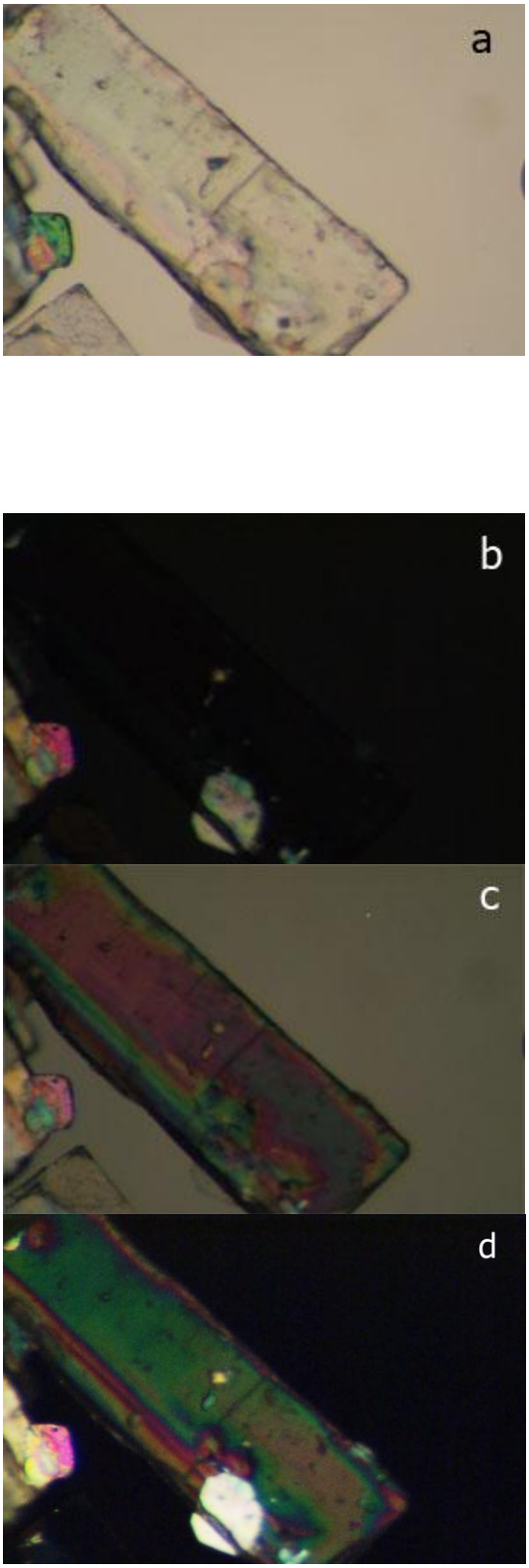

Fig 5.5 *The crystal as seen in the birefringence analysis. The crystal that is meant in the analysis is the large crystal that is oriented at an angle of 45 º.*

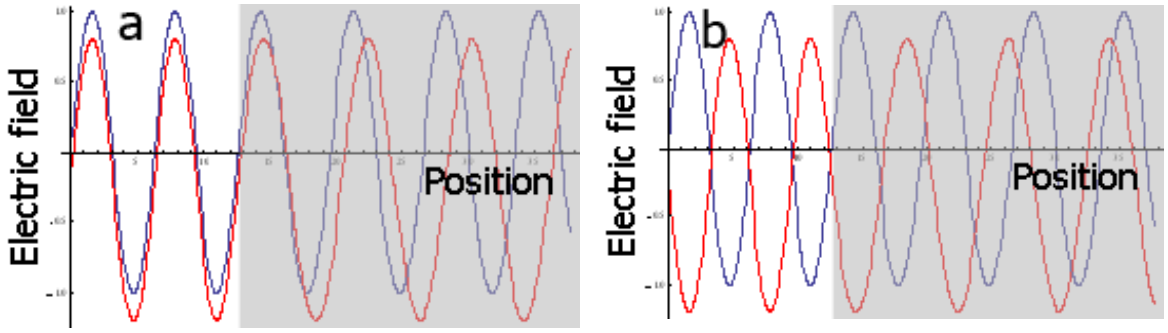

Fig 5.6a *The electric fields of the the light (shown as red (a-axis) and blue (b-axis) sines, with the red shifted down for clarity) are parallel when entering the crystal. When it enters the crystal, one ray is retarded with respect to the other.*
Fig 5.6b *The electric field is exactly out of phase when entering the material, and it stays exacly out of phase with the electric field in 5.6a.*

The colours produced by birefringence are characterized by a Michel-Levy Birefringence Chart given in **fig 5.7**. The birefringence (difference in refractive indices), the thickness of the crystal and the colour are related. In the Mn hybrid the thickness could not be measured exactly and the difference in refractive indices is not known, so no conclusions could be drawn. However, once one of those parameters is known, the colour can give an easy and fast way to determine the thickness or the birefringence. The refractive index is related to the dielectric constant (ε) by $n = \sqrt{\varepsilon}$ [34], so if the difference in dielectric constant is known, the refractive index is also known. However, the difference in dielectric constants is very hard to measure as it is very small.

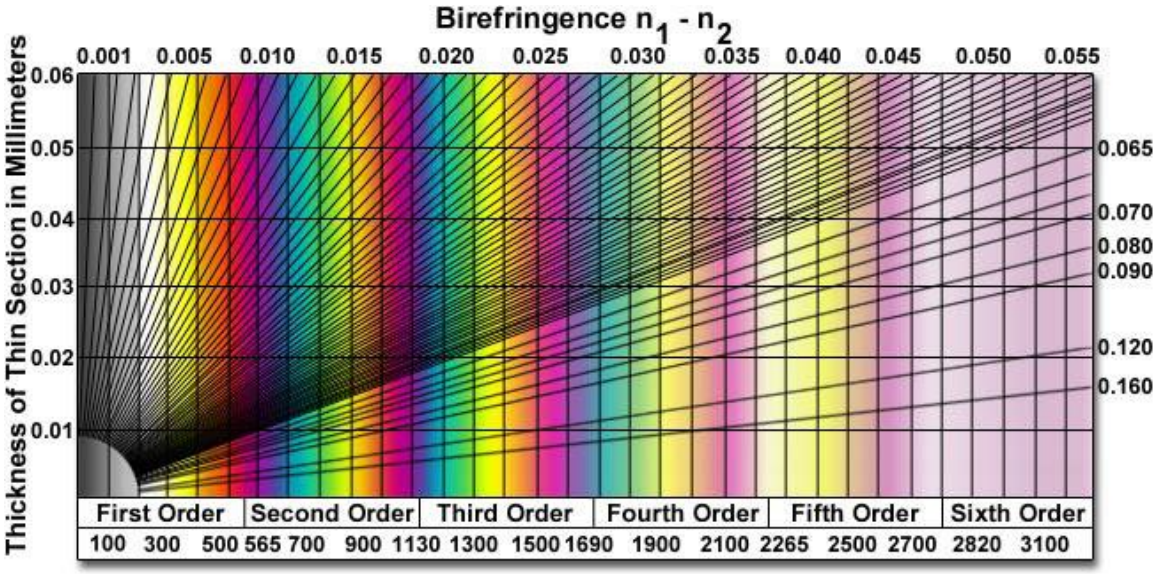

Fig 5.7 [33] *Michel-Levy Birefringence Chart. There are three parameters in this chart: crystal thickness, Birefringence (difference in refractive indices from the two axes) and the colour. When two of the three parameters are known, the third can be identified. The way to read this chart, is to look at the colour and the thickness and then follow the black line for a birefringence. The numbers at the bottom are the retardation of the light in nm.*

The birefringence analysis can be used to identify the axes. As long as it is not known which axis has a higher refractive index, it can not be said which colour is given by which axis, but it can be observed where the axes change. In **fig 5.8** (the cover figure), a typical cluster of crystals of the Mn hybrid is shown, where several changes can be seen in the a- and b-axes.

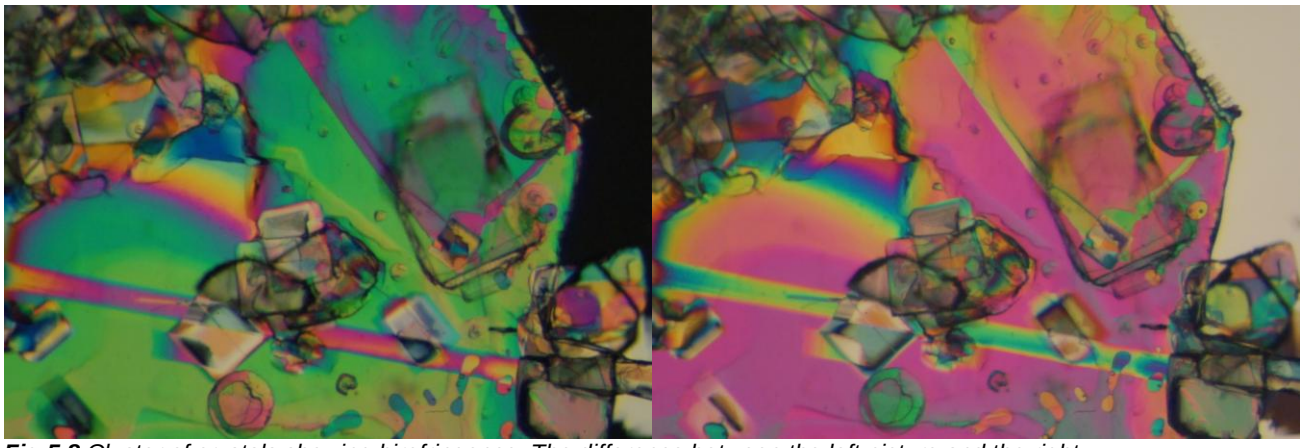

Fig 5.8 *Cluster of crystals showing birefringence. The difference between the left picture and the right picture is a rotation of 90 º of the incoming polarisation.*

The birefringence analysis is performed at a temperature range from room temperature to 160 ºC. The colours changed when the temperature went up, so the birefringence changes with temperature as also observed in literature with other hybrids [13, 35]. At the phase transition at 100 ºC, the birefringence becomes zero as no colours could be observed any more. At the second phase transition, no change could be observed. When cooled down below the first phase transition, birefringence re-appeared, as shown in **fig 5.9**.

The cause of birefringence is a difference in a- and b-axes, so at the phase transition at 100 °C, the difference between those two axes becomes zero. Both axes become equal at that temperature.
In **fig 5.9**, it can be seen that the original a-axis or b-axis oriented domains change after they has been through the phase transition. So the material does not remember which domains it originally had. The domain formation could not be influenced by an external electric field, so the change in a- and b-axes are unlikely to be a cause of polarisation.

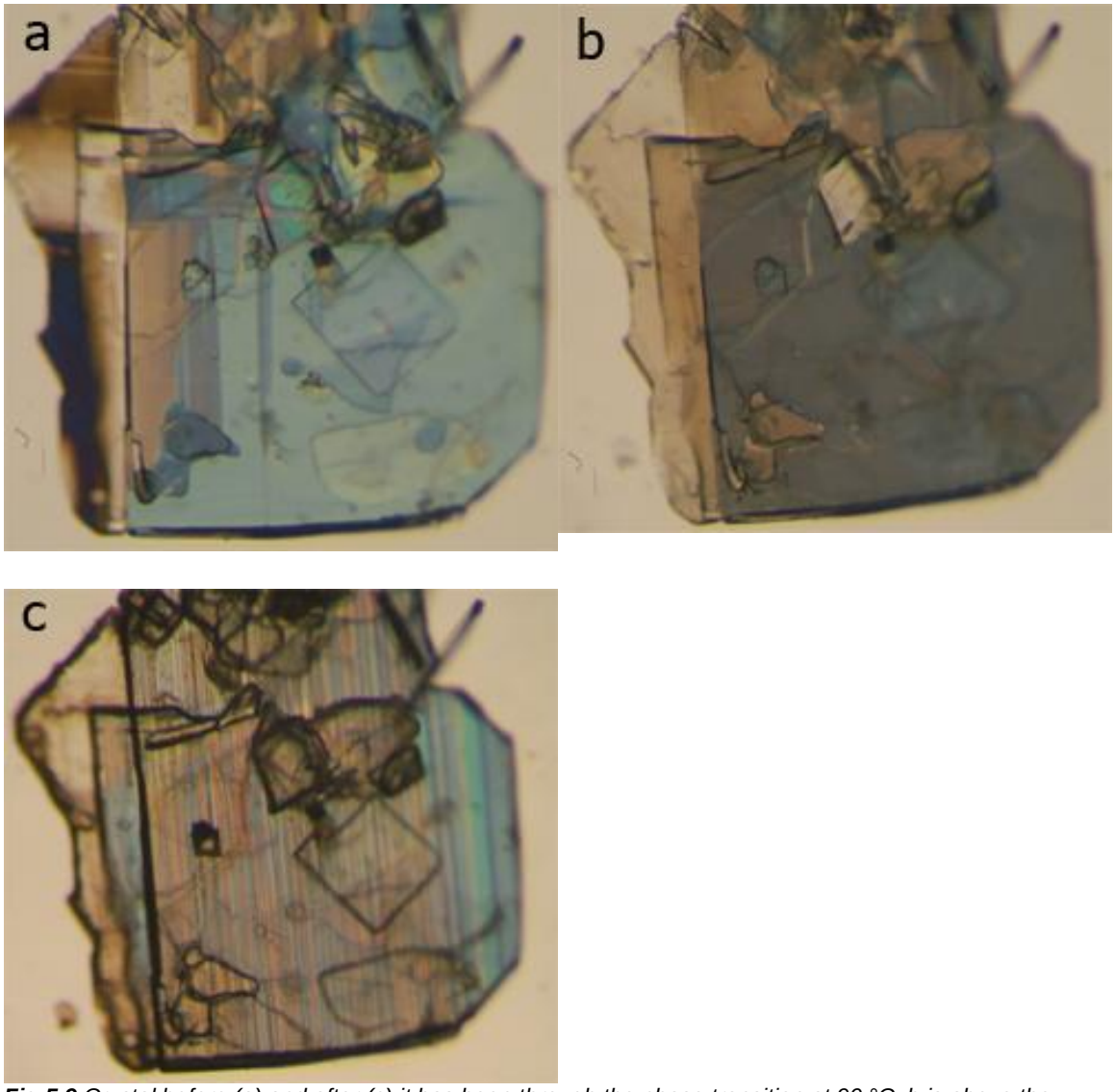

Fig 5.9 *Crystal before (a) and after (c) it has been through the phase transition at 90 °C. b is above the phase transition (110 °C). The colours disappear above the phase transition and the colours re-appear in different domains after it has been cooled down through the phase transition again.*

6. Temperature dependent X-ray

Powder X-ray diffraction has been performed at several temperatures, before and after the phase transition.

Peak shift

The positions of several of the largest peaks has been followed in temperature. From those temperatures, the distances between those planes were calculated using Bragg's Law: $\lambda = 2 d \sin(\theta)$, with λ the wavelength of the X-ray, d the distance between planes and θ the angle [36]. The most notable shift of planes was in the {00x} planes, which were elongated most. The c-axis (plane {001}) was elongated by about 0.06 nm from 30 ºC to 160 ºC. Other planes like {113} did not have such large elongations. In none of the planes, a discontinuity was observed at any of the phase transitions. In **fig 6.1** a percentual graph is shown of the elongation of several planes at several temperatures. This shows that the bonds in the c-axis are the weakest.

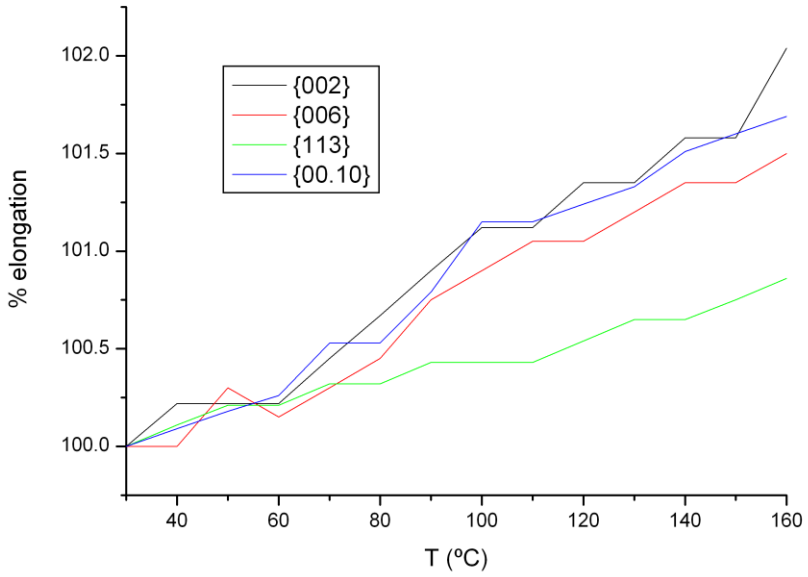

Fig 6.1 *Percentual elongation of several planes. The {113} plane was elongated significantly less than the {00x} planes.*

{020} and {200} planes

The planes {020} and {200} are a representation of the length of the, respectively, b- and a-axes. From the birefringence analysis, it was seen that these axes become equal at the phase transition at 100 ºC and nothing could be observed at 140 ºC. In **fig 6.2**, the reflections of the {020} and {200} planes are given at several temperatures. It can be seen that at the phase transition at 100 ºC, the two reflections form one reflection and are no longer separated. At 140 ºC, there is no change to be observed in any of those axes. So the X-ray confirms that the a- and b-axes become equal at 100 ºC.

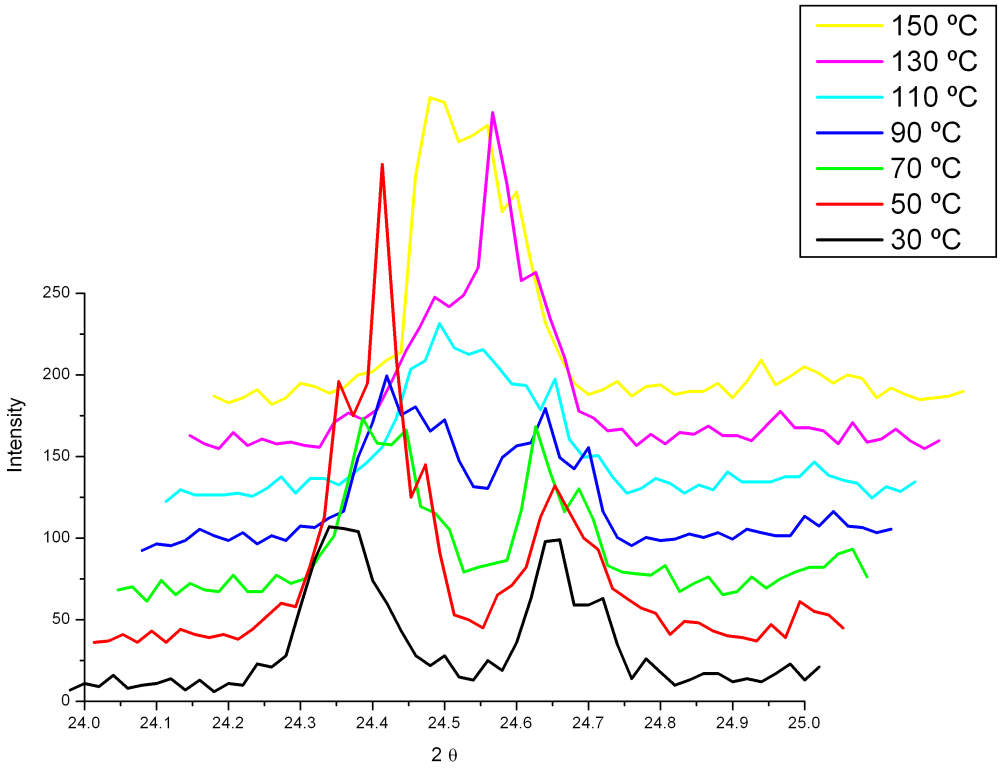

Fig 6.2 *The {020} and {200} planes displayed graphically over a temperature range. At 100 ºC, the difference between the reflections disappear. The peak at lowest angle is the {200} plane.*

Structural changes

Structural changes at phase transitions can be characterised by a change in the distance between certain planes, as can be seen at the {020} and {200} planes at the phase transition at 100 ºC. Another way to see structural changes is by looking at the reflections that are in the spectrum and to see if any reflections appear or disappear, which points to the appearance or disappearance of certain planes. At both the 100 ºC and 140 ºC phase transition, no reflections appeared or disappeared. So for the 100 ºC phase transition, the fact that the a- and b-axes become equal is the only change and for the 140 ºC phase transition there are no structural changes.

7. Capacitance

Capacitance is the ability of a material to hold charge at its surface. The capacitance is related to the dielectric constant, ε, via $C = \varepsilon \varepsilon_0 A / d$ with ε_0 permittivity of vacuum, A the surface and d the thickness. The capacitance is related to the polarisation of a material. The more polar a material is, the more charge it can hold on its surface. This is displayed in **fig 7.1**. A polar material forms dipoles, and these dipoles give an electric field over the material, so charge can build up on the surfaces to compensate that electric field. [37]
When measuring the capacitance, the dielectric loss factor is also measured. This loss can only be caused by conductivity through the sample, so the loss is proportional to the conductivity in the sample. The Mn hybrid is an insulator, so the losses are expected to be low, in the order of magnitude of 0.001. [38]

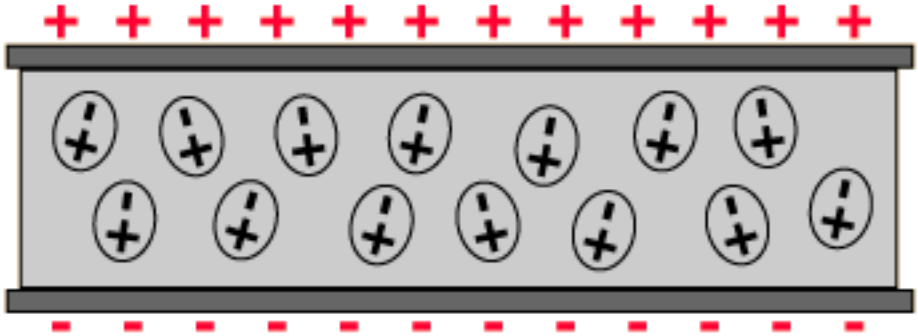

Fig 7.1 *A polar material has dipoles, and if the dipoles are aligned, they form an electic field. This field allows charge to build up on the surface.*

The capacitance of the sample is measured by an Agilent 4284A. The sample is prepared with two contacts, which are placed perpendicular to the c-axis. The crystal is placed on a glass plate with varnish. The contacts were painted on the crystal with silver paint and platinum wires were attached to those silver contacts. This setup is displayed in **fig 7.2**. The thickness of the sample was 0.05mm, the width of the contacts 1.58 mm and the distance between the contacts 2 mm.

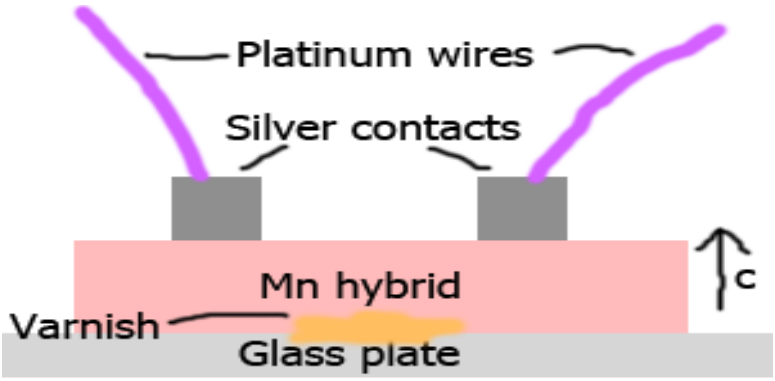

Fig 7.2 *Setup of the contacts on the crystal. The Mn hybrid is oriented with the c axis perpendicular to the glass plate.*

The capacitance was measured at a few frequencies in a temperature scan. The results are displayed in **fig 7.3**. The measurement was done several times for each frequency, and the ones that displayed the characteristics of that frequency best, are shown. For 10

kHz no good measurement was obtained. The capacitance for the 1 kHz measurement was shifted upwards by 1.8 pF to get it in the same window as the other measurements. This can be done because other 1 kHz measurements confirmed that this frequency can yield those values.

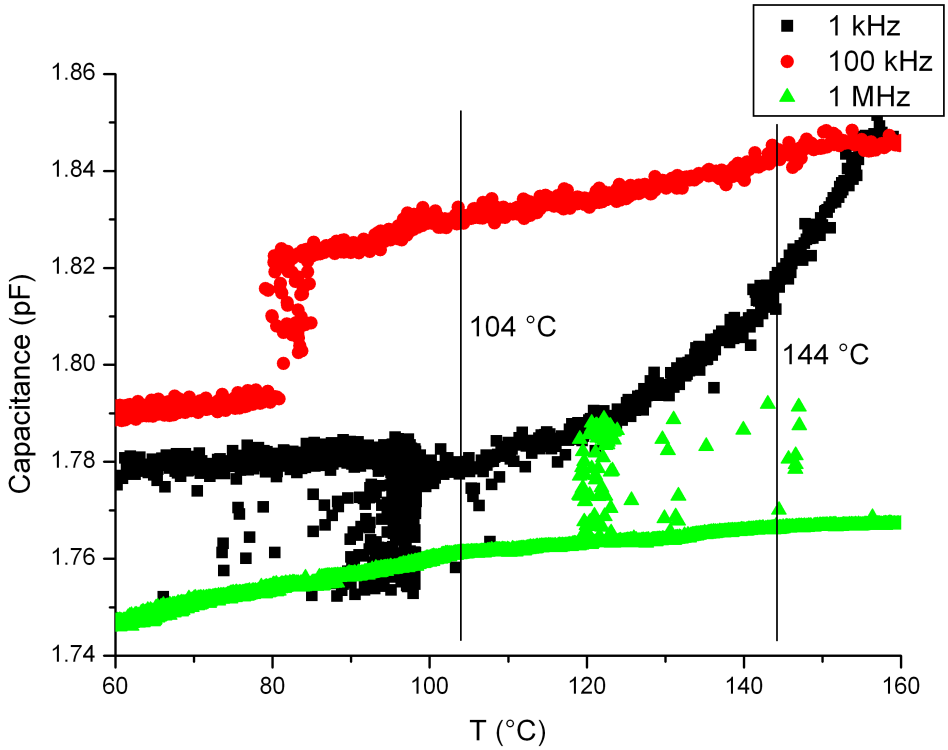

Fig 7.3 *The capacitance in pF versus the temperature for the frequencies 1 kHz, 100 kHz and 1 MHz. The capacitance for 1 kHz was shifted up by 1.8 pF to get it in the same view as the other frequencies. The jump at 80 °C in the 100 kHz frequency is a jump that could not be reproduced. The losses are of the order 0.001 for the 100 kHz and 1 MHz measurement and of the order 1 for the 1 kHz measurement.*

At both phase transitions, a small change in the slope of the dielectric constand could be observed. In **fig 7.4**, these slope changes are given in more detail. The slope changes only little, but they are observable and reproducable. The temperature of the slope change is not exactly the same as the ones in the DSC measurement, but in these capacitance measurements, the temperature was not registered very accurately. This gives the clue that the polarisation is changing in the material at 144 °C. That phase transition is a phase transition as observed by the DSC measurement, and since there is no structural transition, it must be another parameter, with the polarisation being a very good candidate. The slope change at 100 °C is probably due to the structural change.

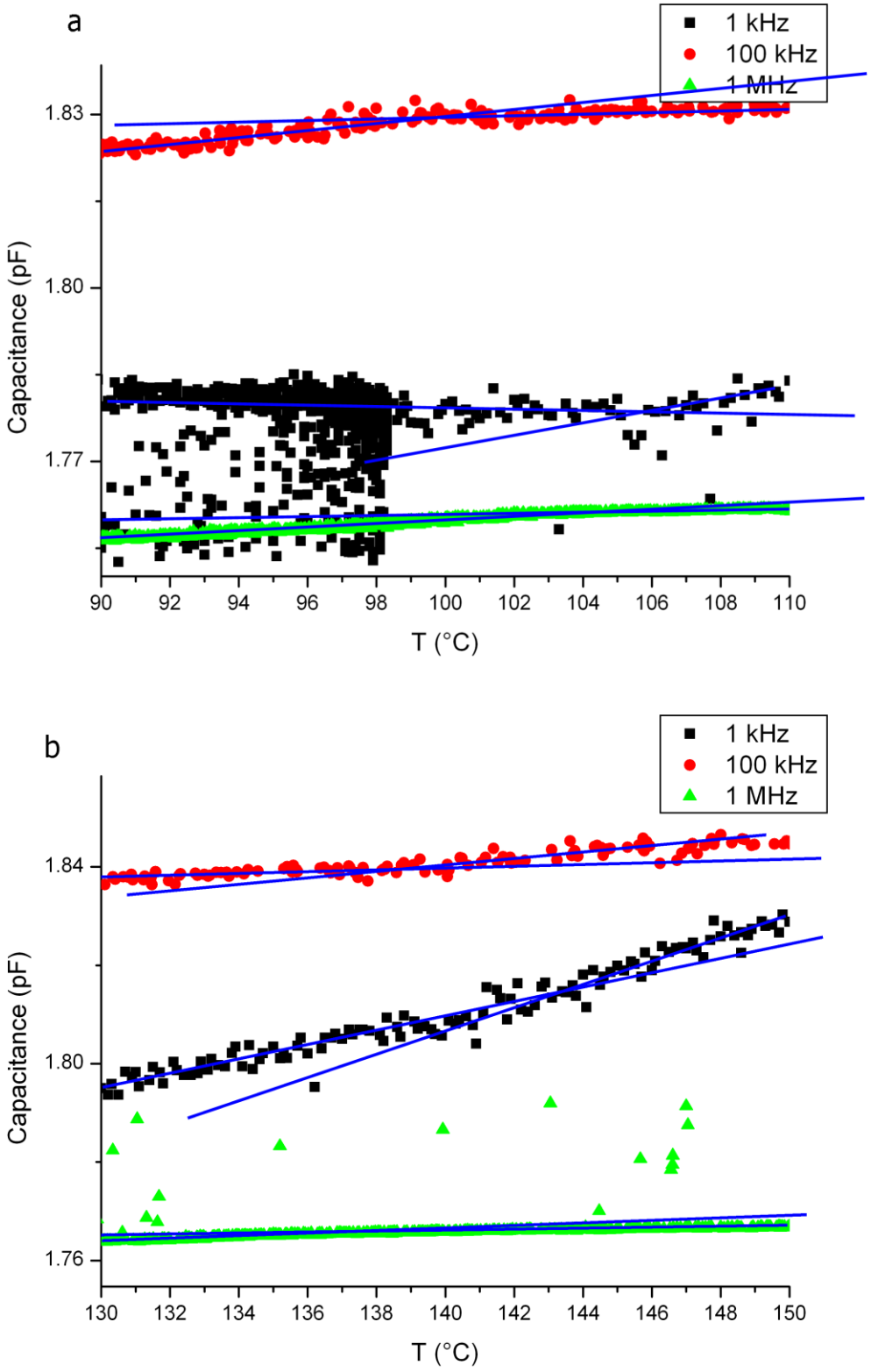

Fig 7.4 *Details of the capacitance measurements. In a, the slope changes of the capacitance at the phase transition at 100 °C is shown, and in b, the slope changes for the 144 °C phase transition is shown.*

The losses are as expected for the 100 kHz and 1 MHz measurements: fairly low as the Mn hybrid is an insulator. The losses for the 1 kHz measurement are unexpectedly high. The curve of the loss value is also very interesting (**fig 7.5**), as it shows a peak at the second phase transition. This will be covered in chapter 8. The loss values of the other frequencies in the temperature scan showed continuous curves without slope changes. So the conductivity is not changed at the phase transitions.

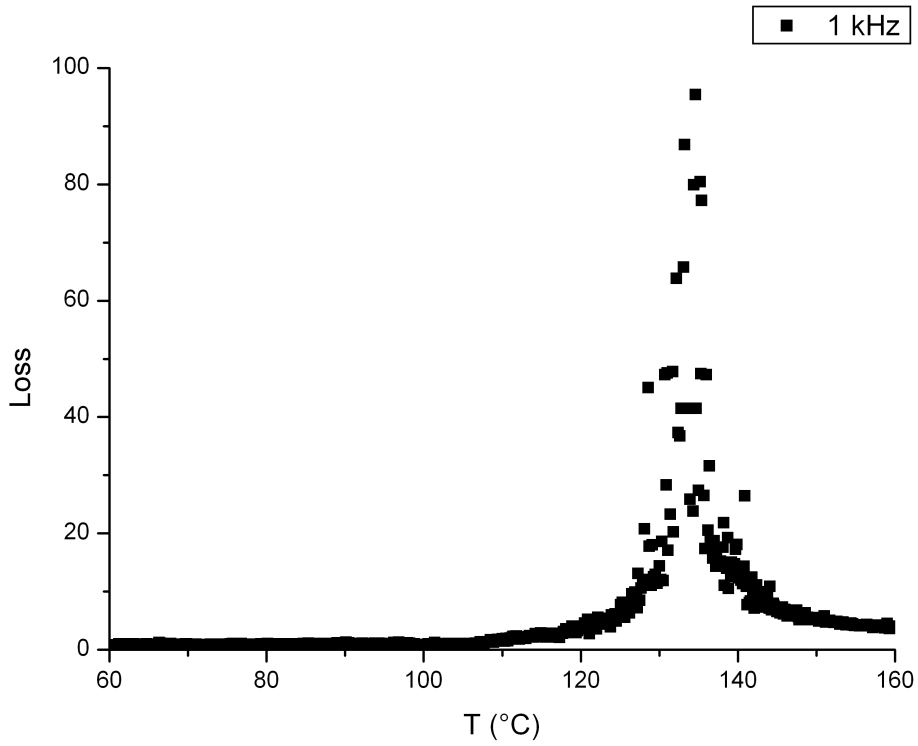

Fig 7.5 *Losses for the 1 kHz sample during the capacitance measurement.*

8. Pyroelectric current

A pyroelectric current is the creation of a current when a sample is heated through a phase transition. The origin of this current is a polar phase and it is shown schematically in **fig 8.1**. Blow the phase transition, the material is polar. The dipoles are aligned to give a macroscopic electric field. Because of this field, a charge is built up on the surfaces to compensate this electric field, producing a neutral state. When the material is heated to an unpolar phase through the phase transition, the polarisation in the sample is lost. There are two mechanisms for losing the polarisation: the dipoles become neutral (**fig 8.1a**) or the dipoles get randomly oriented (**fig 8.1b**), the order-disorder effect.
When the material loses its polarisation, the charge on the surface can be registered as a current. A current peak is expected just before the phase transition, because the material relaxes before the phase transition and all charge is gone at the phase transition.

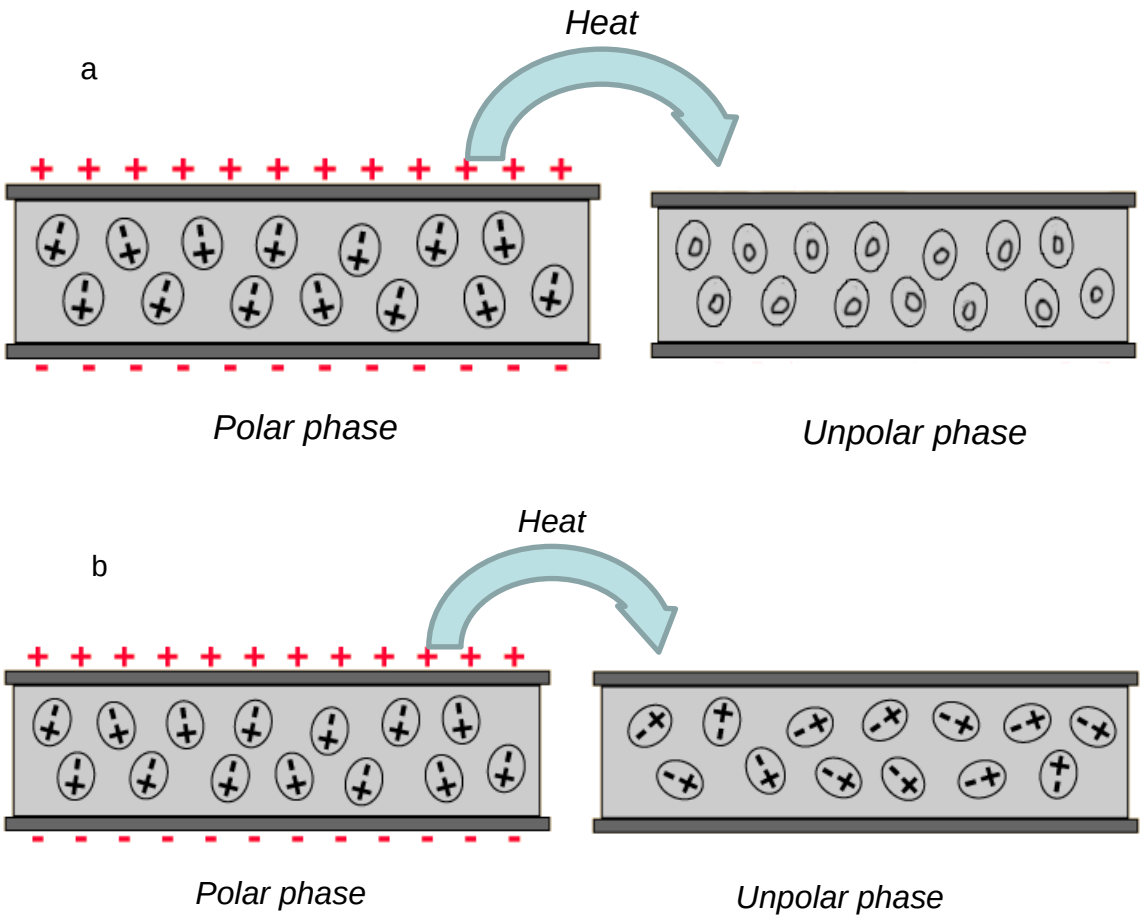

Fig 8.1 *[39] Pyroelectric current measurement. The material is in a polar phase and under heating it becomes unpolar. That is possible by two mechanisms: dipoles become neutral (a) or the dipoles become randomly ordered (b – order-disorder effect).*

The setup and the same crystal of **fig 7.2** was used to measure the pyroelectric current. First, the sample was heated to 160 °C, which is above both phase transitions. A voltage was applied by a Keithley 6517A over the material which created an electric field of 200

kV/m. The material was cooled down through the phase transitions while applying that voltage. After the material was cooled down below the phase transitions, the electric field was switched off and the current was measured by the Keithley 6517A. The current was measured while the sample was heated up to 160 °C. The results are given in **fig 8.2**. A peak in the current can be seen just before the second phase transition at 144 °C. An exponential looking background was observed and the origin of it is not expected as there is no voltage applied. It is not known what the origin of the back ground is, and it can not be a thermoelectric effect. If there was a thermoelectric effect between the Mn hybrid and any part of the circuit, there is a voltage built up between those two elements. But this voltage would also be built up at the other side of the circuit, which is an exact opposite voltage. These two voltages cancel out each other.
In the dielectric measurement of chapter 7, at 1 kHz the loss value showed a typical pyroelectric current (given in **fig 7.4** and **fig 8.3**). This loss is proportional to the conductivity, which would mean the conductivity of the material shows a peak at the place of the pyroelectric current. But this is not true, since the conductivity is not effected by pyroelectricity. And from the loss values at the other frequencies of the capacitance measurement is can be seen that the conductivity does not change discontinuously at the phase transitions.
Conductivity is measured by the amount of current at a certain voltage. In the pyroelectric effect, there is a current generated by the heating, without any voltage change. So the peak in the loss value in **fig 8.3** is not due to true conductivity, but due to another supply of current, of which the apparatus thinks it's a loss. This other supply of current is the pyroelectric current.
This current was only observed at a frequency of 1 kHz and not at higher frequencies. So the cause of polarisation in the Mn hybrid is able to lose its polarisation to fields up to 1 kHz, but not able to lose its polarisation to fields of 100 kHz and higher.

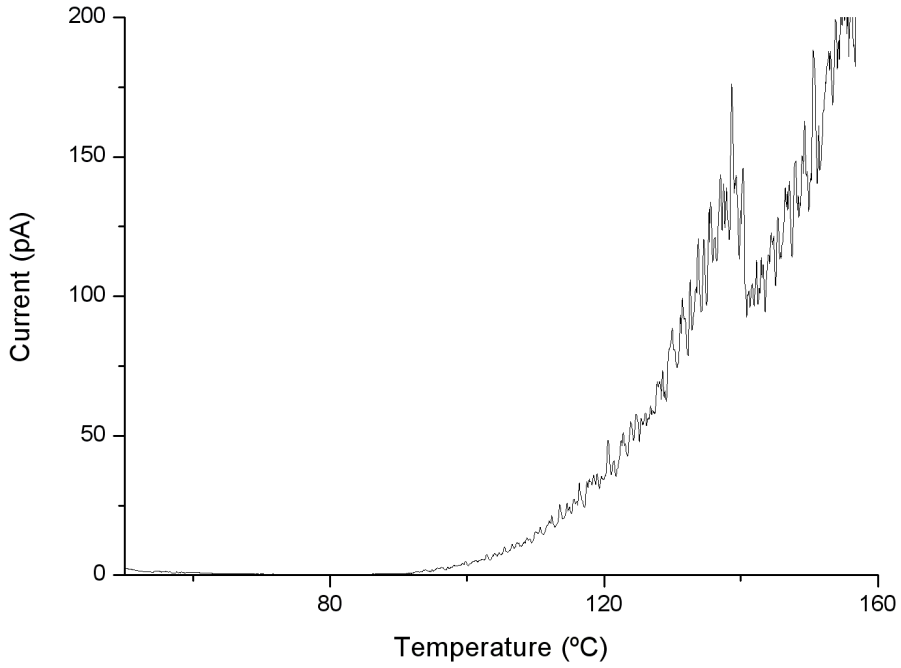

Fig 8.2 *Temperature versus the current, a pyroelectric current could be observed just before the second phase transition at 144 °C.*

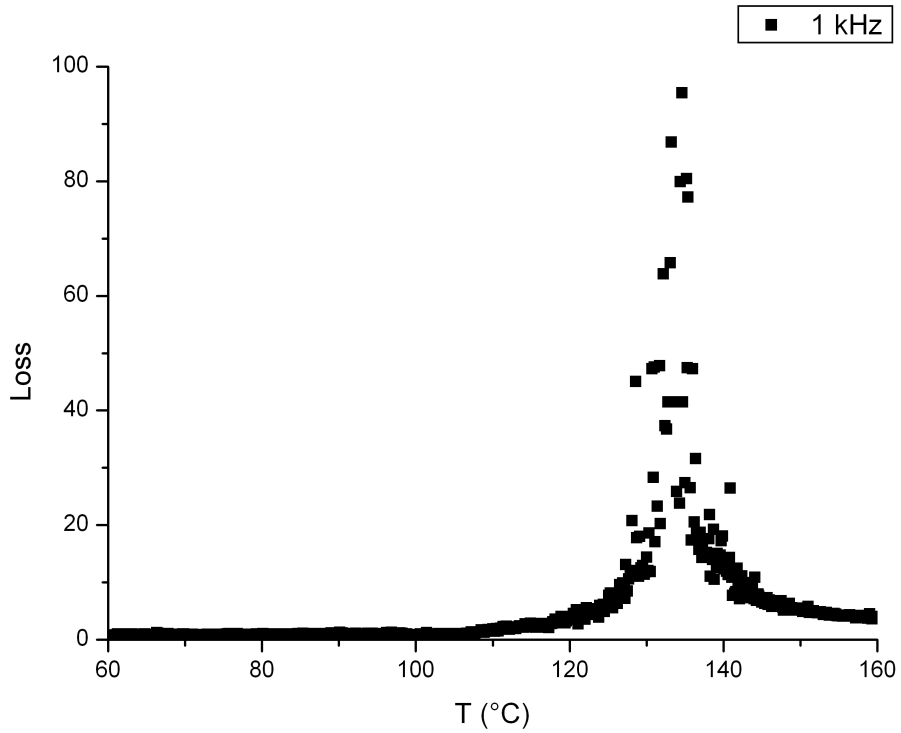

Fig 8.3 *The temperature versus the loss value for capacitance measurements at 1 kHz. The loss value shows characteristic pyroelectric beheavior.*

The current (I) can be integrated with respect to time (t) to produce charge (Q) on the surface: I * t = Q. An exponential function is fitted to the background in **fig 8.2**, and then the current was integrated over time. A charge of 5.52 nC was found, which is the amount of charge that was on the surface before the phase transition.
This charge can be converted into the polarisation of the material. The surface where a charge is built up, is the surface perpendicular to the contact: the thickness of the crystal * the width of the contact. This is 0.05 mm * 1.58 mm = 0.079 mm^2. The polarisation (P) of the material is the amount of charge (Q) on a surface (A): P = Q / A = 6.99 $\mu C/cm^2$. This value is of the same order of magnitude as organic or hybrid ferroelectrics like Thiourea or TGS [40] and two orders of magnitude larger than the Cu hybrid [1].

If the nitrogen is the cause of polarisation, the displacement of it can be calculated with this value. The displacement (l) * the charge (Q) of the nitrogens (2 times elementary charge) in a unit cell is the dipolar moment (p). This dipolar moment is the polarisation (P) * volume of one unit cell (V). The volume of one unit cell is 2.02 * 10^{-27} m^3. So P * V = p = 1.41 * 10^{-28} Cm and l = p / Q = 4.41 Á. Such a displacement of the nitrogens would give a shift of 4.9 ° in the powder X-ray spectrum for a plane which contains nitrogens, which is not observed (chapter 6). So a displacement of the nitrogens is not the cause of the polarisation in the sample.

This pyroelectric current shows that the second phase transition at 144 °C is a polar phase transition. However, it does not prove yet that the material is a pyroelectric or a ferroelectric. To prove it is a pyroelectric, the pyroelectric current must be able to be reversed. The direction of the dipoles must be able to be changed by an external electric

field. However, the pyroelectric current has only been measured twice out of many times that it was tried and the electric field was not reversed in those cases. So more experiments are needed to prove it is a pyroelectric.
To prove it is a ferroelectric, this external field must be applied in the polar phase (to produce a ferroelectric hysteresis loop). It has been tried to measure the ferroelectric hysteresis loop, but the field applied was not large enough and the leakage (the losses in the capacitance measurement) was too high at low frequency of the capacitance. A proof it is ferroelectric could not be given as a hysteresis loop could not be measured. But these experiments did yield the fact that the second transition is a polar phase transition with a polarisation that is similar to other hybrid ferroelectrics, so there is a good chance the Mn hybrid can still show ferroelectricity.

9. Conclusions

Phase transition at 100 ºC

In the Mn hybrid, in the range of -100 ºC to +200 ºC two phase transitions are proven by DSC: a second order phase transition at 100 ºC and a first order phase transition at 144 ºC. The first phase transition at 100 ºC is a structural phase transition. In the crystal structure, the a- and b-axes below the phase transition are different because the a-axis has buckling in the octahedra and the b-axis is not buckled. At the phase transition of 100 ºC, the two axes become the same, as can be seen by birefringent analysis (chapter 5) and the X-ray spectrum (chapter 6). From those analyses it could not be extracted what that structure becomes after the phase transition, but it can be assumed that the buckling disappears. Arguments for the disappearance is that the buckling disappears in the Cu hybrid at higher temperature [1], and from entropic arguments it can be deducted that it is most logical that the buckling disappears: the freedom of the material is very low in the buckled state, while the freedom gets larger when it is flat (more possible conformations). Higher temperature favours the entropically more stable systems (entropy is temperature dependent in the Gibbs energy [41]). The only real proof can be given by single-crystal X-ray diffraction above the phase transition.
This phase transition does not seem to include a change in polarisation. The pyroelectric measurement did not give any results for this phase transition and the capacitance measurement gave a slope change in the capacitance, but that could very well be explained by the change in structure. If the buckling was the cause of polarisation, the buckling should be able to be influenced by an external electric field. The birefringent analysis showed that an external field had no influences on the orientation of the axes. So in contrast with the Cu hybrid [1], the Mn hybrid does not get polarisation from the buckling of the octahedra.

Phase transition at 144 ºC

The phase transition at 144 ºC does not have any observable structural change in the X-ray spectrum. It is a first order phase transition as proven by the DSC, so there must be a change in one of the thermodynamic parameters.
A slope change in the capacitance at this phase transition seems to point to the fact that this phase transition has something to do with polarisation, as polarisation influences capacitance. The pyroelectric current measurement confirms that this phase transition is a transition from a polar to an unpolar phase.
The origin of the polarisation is not known. It can not be a shift of the nitrogen atoms. The nitrogen atoms need to shift with 4.4 Å, and then a plane with the nitrogens is shifted 4.9 ° in the powder X-ray spectrum, which is not observed for any plane. The origin of the polarisation can lose its polarisation with oscillating fields up to 1 kHz, but not anymore at fields of 100 kHz or more. Since the capacitance at all those fields have more or less the same slope change, it can be concluded that the permanent polarisation of the material can follow fields up to 1 kHz, while the temporary polarisation can follow any field.
The material is not proven to be pyroelectric or ferroelectric. For ferroelectricity, a ferroelectric loop is required but that could not be measured, even though it does not mean it's not there. The polarisation is of the same order of magnitude as some organic or hybrid ferroelectrics, so the Mn hybrid has good chance to be ferroelectric.
For further research, it is most important to find the origin of polarisation. An important clue could be found if the crystal structure above the second phase transition is known.

Something else that must be done, is to find out if the material is true pyroelectric by getting a pyroelectric current while the material is poled into the other direction.

Multiferroicity

The Mn hybid has already been proven to be antiferromagnetic [1], and it is proven to be polar. It is hard to prove if it is ferroelectric, but more clues can be found if the origin of polarisation is known. The polarisation is of the order of magnitude as other ferroelectrics, so the Mn hybrid has good potential to be a multiferroic.

10. Literature

[1] A.H. Arkenbout, PhD thesis (in preparation)
[2] D.B. Mitzi, "*Synthesis, structure and Properties of Organic-Inorganic Perovskites and Related Materials*", Progress in Inorganic Chemistry, **48**, 1 (1999)
[3] D.B. Mitzi, "*Synthesis, Crystal Structure, and Optical and Thermal Properties of* $(C_4H_9NH_3)_2MI_4$ *(M = Ge, Sn, Pb)*", Chem. Mater., **8**, p. 791-800 (1996)
[4] I. Zarezba-Grodz, W. Mista, W. Strezk, E. Bukowska, K Hermanowicz, K. Maruszewski, "*Synthesis and properties of an inorganic–organic hybrid prepared by the sol–gel method*", Optical Materials, **26**, p. 207–211 (2004)
[5] P. Jain et al., "*Multiferroic Behavior Associated with an Order-Disorder Hydrogen Bonding Transition in Metal-Organic Frameworks (MOFs) with the Perovskite* ABX_3 *Architecture*", Journal of American Chemical Society, **131**, p. 13625–13627 (2009)
[6] C. Aruta, F. Licci, A. Zappettini, F. Bolzoni, F. Rastelli, P. Ferro, T. Besagni, "*Growth and optical, magnetic and transport properties of* $(C_4H_9NH_3)_2MCl_4$ *organic-inorganic hybrid films (M = Cu, Sn)",* Appl. Phys. A, **81**, p. 963–968 (2005)
[7] W. Zhou, T Yildirim, "*Nature and Tunability of Enhanced Hydrogen Binding in Metal-Organic Frameworks with Exposed Transition Metal Sites*", Journal of physical chemistry C, **112**, 8132–8135 (2008)
[8] P. Gomez-Romero, "*Hybrid Organic-Inorganic Materials In Search of Synergic Activity*", Adv. Mater., **13**, 3 (2001)
[9] K. Baberschke, F. Rys, "Chloride *Perovskite Layer Compounds of* $[NH_3\text{-}(CH_2)_n\text{-}NH_3]MnCl_4$ *Formula*", Solid State Communications, **18**, p. 999-1003 (1976)
[10] H. Arend, W. Huber, *"Layer Perovskites of the* $(C_nH_{n+2}NH_3)_2MX_4$ *and* $NH_3(CH_2)mNH_3MX_4$ *Families with M=Cd, Cu, Fe, Mn or Pd and X=Cl or Br: Importance, solubilities and simple growth techniques*", Journal of Crystal Growth, **43**, p. 213-223 (1978)
[11] Z.T. Jiang et al., "Investigation of the ferroelectric phase transition in $CH_3NH_3HgCl_3$", J. Phys. Chem. Solids, 56. p. 277-283 (1995)
[12] J.J. Foster, N.S. Gill, *"Complex halides of the transition metals. Part III. Electronic spectra and ligand field parameters of octahedral and tetrahedral halogeno-complexes of manganese(II)"*, Journal of the Chemical Society A: Inorganic, Physical, Theoretical, pp. 2625-2629 (1968)
[13] K. Knorr, I.R. Jahn, G. Heger, "*Birefringence, X-ray and neutron diffraction measurements on the structural phase transitions of* $(CH_3NH_3)_2MnCl_4$ *and* $(CH_3NH_3)_2FeCl_4$", Solid State Communications, **15**, p. 231-238 (1974)
[14] R. Ramesh, "*Emerging routes to multiferroics*", Nature, **461**, p. 1218-1219 (2009)
[15] N. A. Hill, "*Why Are There so Few Magnetic Ferroelectrics?*", J. Phys. Chem., **104**, 6694-6709 (2000)
[16] W. Eerenstein, N. D. Mathur, J. F. Scott, "*Multiferroic and magnetoelectric materials*", Nature, **442**, p. 759-765 (2006)
[17] http://hyperphysics.phy-astr.gsu.edu/hbase/electric/dielec.html
[18] http://en.wikipedia.org/wiki/Ferroelectricity
[19] N. A. Hill, A. Filippetti, "*Why are there any magnetic ferroelectrics?*", Journal of Magnetism and Magnetic Materials, **242–245**, p. 976–979 (2002)
[20] S. Cheong, M. Mostovoy, "*Multiferroics: a magnetic twist for ferroelectricity*", Nature materials, **6**, p. 13-20 (2007)
[21] K.F. Wang, J.M. Liu, Z.F. Ren, "*Multiferroicity: the coupling between magnetic and polarization orders*", Advances in Physics, **58**, p. 321–448 (2009)

[22] G. F. Needham, R. D. Willett, H. F. Franzen, "*Phase Transitions in Crystalline Models of Bilayers. 1. Differential Scanning Calorimetric and X-ray Studies of* $(C_{12}H_{25}NH_3)_2MCI_4$ *and* $(C_{14}H_{29}NH_3)_2MCI_4$ *Salts (M =* Mn^{2+}, Cd^{2+}, Cu^{2+})", J. Phys. Chem., **88**, p. 674-680 (1984)
[23] A. H. Arkenbout, A. Meetsma, T. T. M. Palstra, *"(2-Phenylethyl)ammonium chloride*", Acta Crystallographica Section E, **63**, o2987 (2007)
[24] http://www.xrd.us/technote/preferred%20orientation.htm
[25] P. Atkins, "*Physical Chemistry*", 8th edition, p129-131 (2006)
[26] http://www.chem.neu.edu/Courses/1382Budil/PhaseBehaviorPureCompounds.htm
[27] P. Atkins, "*Physical Chemistry*", 8th edition, p42 (2006)
[28] K. Horiuchi, "Structural *Phase TRansitions in (C2H5NH3)2- and (n-C4H9NH3)2ZnBr*", Journal of the Physical Society of Japan, **63**, 363-364 (1994)
[29] G.F. Needham, R.D. Willett, H.F. Franzen, "*Phase Transitions in Crystalline Models of Bilayers. 1. Differential Scanning Calorimetric and X-ray Studies of* $(C_{12}H_{25}NH_3)_2MCI_4$ *and* $(C_{14}H_{29}NH_3)_2MCI_4$ *Salts (M =* Mn^{2+}, Cd^{2+}, Cu^{2+})", Journal of Physical Chemistry, **88**, 674-680 (1984)
[30] J.P. Patel, A. Singh, D. Pandey, "*Nature of ferroelectric to paraelectric phase transition in multiferroic 0.8 BiFeO3-0.2Pb (Fe1/2Nb1/2)O3 ceramics*", Journal of Applied Physics, **107**, 104115 (2010)
[31] V.B. Sajfert, Lj.D. Maskovic, R.P. Djajic-Jovanovic, U.F. Kozmidis-Luburic, "*Phase transition in 1D KDP-type ferroelectrics*", Physica Status Solidi (B) Basic Research, **148**, 81-90 (1988)
[32] http://spot.pcc.edu/~aodman/physics%20122/light-electro-pictures/light-electro-lecture.htm
[33] http://micro.magnet.fsu.edu/optics/lightandcolor/birefringence.html
[34] R. Turton, "*The physics of solids*", 1st edition, p. 287 (2000)
[35] S. H Wemple, M. Didomenico, I. Camlibel, "*Dielectric and optical properties of melt-grown* $BaTiO_3$", J. Phys. Chem. Solids, **29**, p. 1797-1803 (1968)
[36] R. Turton, "*The physics of solids*", 1st edition, p. 55 (2000)
[37] R. Turton, "*The physics of solids*", 1st edition, chapter 10 (2000)
[38] G. L. Johnson, "Lossy capacitors", Solid State Tesla Coil (2001)
[39] http://hyperphysics.phy-astr.gsu.edu/hbase/electric/dielec.html
[40] S. Horiuchi, Y. Tokura, "*Organic ferroelectrics*", Nature materials, **7**, p. 357-366 (2008)
[41] P. Atkins, "*Physical Chemistry*", 8th edition, p94-100 (2006)